

AD-A250 597



MISCELLANEOUS PAPER SL-92-2

2

BRICK MODEL TESTS OF SHALLOW UNDERGROUND MAGAZINES

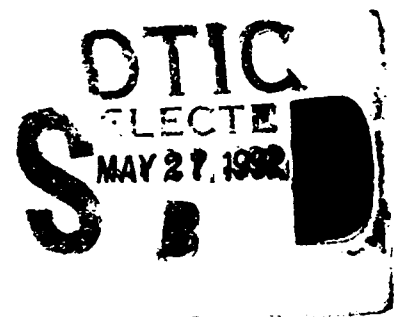
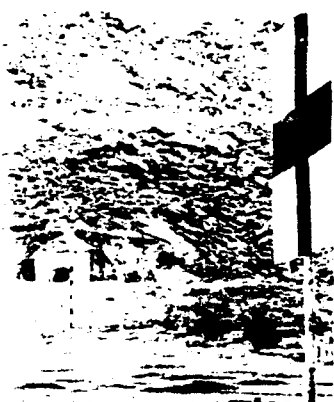
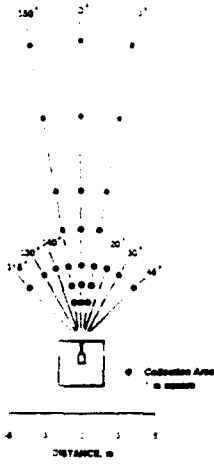
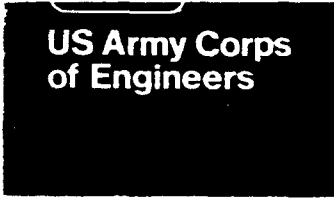
by

Charles E. Joachim, George S. Rubin de la Borboila

Structures Laboratory

DEPARTMENT OF THE ARMY

Waterways Experiment Station, Corps of Engineers
3909 Halls Ferry Road, Vicksburg, Mississippi 39180-6199



March 1992

Final Report

Approved For Public Release. Distribution is unlimited.

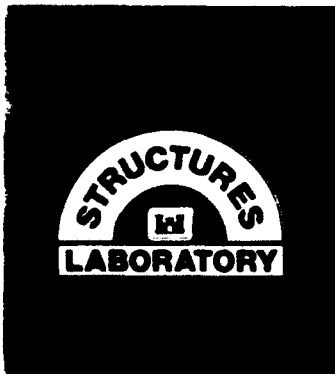
92-13874

Prepared for US Department of Defense Explosives Safety Board

Directorate of Health and Safety
Ministry of Defence, United Kingdom

Norwegian Defence Construction Service

92 5 26 089



Destroy this report when no longer needed. Do not return
it to the originator.

The findings in this report are not to be construed as an official
Department of the Army position unless so designated
by other authorized documents.

The contents of this report are not to be used for
advertising, publication, or promotional purposes.
Citation of trade names does not constitute an
official endorsement or approval of the use of
such commercial products.

REPORT DOCUMENTATION PAGE			Form Approved OMB No. 0704-0188	
Public reporting burden for this collection of information is estimated to average 1 hour per response, including the time for reviewing instructions, searching existing data sources, gathering and maintaining the data needed, and completing and reviewing the collection of information. Send comments regarding this burden estimate or any other aspect of this collection of information, including suggestions for reducing this burden, to Washington Headquarters Services, Directorate for Information Operations and Reports, 1215 Jefferson Davis Highway, Suite 1204, Arlington, VA 22202-4302, and to the Office of Management and Budget, Paperwork Reduction Project (0704-0188), Washington, DC 20503.				
1. AGENCY USE ONLY (Leave blank)	2. REPORT DATE March 1992	3. REPORT TYPE AND DATES COVERED Final Report		
4. TITLE AND SUBTITLE Brick Model Tests of Shallow Underground Magazines			5. FUNDING NUMBERS	
6. AUTHOR(S) Charles E. Joachim George S. Rubin de la Borbolla				
7. PERFORMING ORGANIZATION NAME(S) AND ADDRESS(ES) USAE Waterways Experiment Station Structures Laboratory 3909 Halls Ferry Road Vicksburg, MS 39180-6199			8. PERFORMING ORGANIZATION REPORT NUMBER Miscellaneous Paper SL-92-2	
9. SPONSORING / MONITORING AGENCY NAME(S) AND ADDRESS(ES) US DOD Explosives Safety Board Hoffman Building 1 2461 Eisenhower Avenue Alexandria, VA 22331-0600			10. SPONSORING / MONITORING AGENCY REPORT NUMBER	
11. SUPPLEMENTARY NOTES Available from National Technical Information Service, 5285 Port Royal Road, Springfield, VA 22161				
12a. DISTRIBUTION / AVAILABILITY STATEMENT Approved for public release; distribution is unlimited			12b. DISTRIBUTION CODE	
13. ABSTRACT (Maximum 200 words) A series of 1:25-scale model tests in a brick test bed were conducted to investigate the airblast and debris hazards from accidental explosions in shallow underground magazines in jointed rock. The results demonstrated that the blast effects produced in a large-scale test of a shallow magazine could be reproduced with reasonable accuracy in a 1:25-scale model. The model tests also provided an experimental basis for extending the results of the large-scale test to account for variations in the thickness and strength of the rock cover and in the chamber loading density.				
14. SUBJECT TERMS Ammunition storage Explosives safety Accidental explosions			15. NUMBER OF PAGES 81	
			16. PRICE CODE	
17. SECURITY CLASSIFICATION OF REPORT Unclassified	18. SECURITY CLASSIFICATION OF THIS PAGE Unclassified	19. SECURITY CLASSIFICATION OF ABSTRACT	20. LIMITATION OF ABSTRACT	

PREFACE

The model test program reported herein was performed by the Explosion Effects Division (EED), Structures Laboratory (SL), of the U.S. Army Engineer Waterways Experiment Station (WES), during the period 1 July 1989 through 30 December 1990. The investigation was sponsored by the U.S. Department of Defense Explosives Safety Board (DDESB), the Norwegian Defence Construction Service (NDCS), and the Directorate of Health and Safety (DHS), Ministry of Defence, United Kingdom.

The program monitors were Dr. C. E. Canada, DDESB, Mr. A. Jenssen, NDCS, and Mr. Jon Henderson, Explosives Storage and Transport Committee, DHS.

The Program Manager for this study was Mr. Charles E. Joachim. Mr. George S. Rubin de la Borbolla was the Project Engineer and conducted the tests, and Messrs. Joachim and Rubin prepared this report. Other EED personnel assisting in the study were Messrs. D. F. Hale, R. N. Walters, and G. E. Phillips. Mr. C. N. Thompson, WES Instrumentation Services Division, provided instrumentation and data recording support. Mr. Eugene J. James, WES Engineering and Construction Services Division, assisted with model construction.

The work was performed under the general supervision of Mr. L. K. Davis, Chief, EED, and Mr. Bryant Mather, Chief, SL.

Dr. Robert W. Whalin was Director of WES. COL Leonard G. Hassell, EN, was Commander and Deputy Director.



Accession For	
NTIS GRA&I	<input checked="" type="checkbox"/>
DTIC TAB	<input type="checkbox"/>
Unannounced	<input type="checkbox"/>
Justification _____	
By _____	
Distribution/	
Availability Codes	
Dist	Avail and/or Special
A-1	

CONTENTS

	Page
PREFACE.....	i
LIST OF FIGURES.....	iii
LIST OF TABLES.....	v
CONVERSION FACTORS, SI (METRIC) TO NON-SI UNITS OF MEASUREMENTS.....	vi
SECTION 1 INTRODUCTION.....	1
1.1 BACKGROUND.....	1
1.2 OBJECTIVE.....	2
SECTION 2 PROCEDURES.....	3
2.1 APPROACH.....	3
2.2 MODEL CONSTRUCTION.....	3
2.3 INSTRUMENTATION.....	4
2.4 EXPLOSIVE CHARGES.....	5
2.5 EJECTA/DEBRIS COLLECTION.....	6
SECTION 3 RESULTS AND DISCUSSION.....	7
3.1 AIRBLAST EFFECTS.....	7
3.2 DEBRIS EFFECTS.....	10
SECTION 4 CONCLUSIONS AND RECOMMENDATIONS.....	14
4.1 CONCLUSIONS.....	14
4.2 RECOMMENDATIONS.....	14
REFERENCES.....	16
APPENDIX A: AIRBLAST AND GROUND MOTION WAVE FORMS, TEST 1.....	40
APPENDIX B: AIRBLAST AND GROUND MOTION WAVE FORMS, TEST 2.....	49
APPENDIX C: AIRBLAST AND GROUND MOTION WAVE FORMS, TEST 3.....	64

LIST OF FIGURES

<u>Figure No.</u>	<u>Page</u>
1. Access tunnel cross section for 1:25-scale Brick Model Tests.....	17
2. Storage chamber cross section for 1:25-scale Brick Model Tests...	17
3. Layout (centerline profile) of 1:25-scale Brick Model.....	18
4. Testbed design for 1:25-scale tests	19
5. Tunnel portals and foreground areas of the large-scale Shallow Underground Test and the corresponding Brick Model Test.....	20
6. 1.27-kg explosive charge before insertion into chamber of Brick Model Test.....	21
7. Brick Model Test 3: location of ejecta collection areas.....	22
8. Scaled arrival time versus scaled distance from the charge initiation point.....	23
9. Free-field side-on overpressure scaled to the Shallow Underground Tunnel/Chamber Explosion Test parameters.....	24
10. Peak side-on overpressure versus horizontal distance from the charge initiation point.....	25
11. Peak side-on impulse versus horizontal distance from the charge initiation point.....	26
12. Pressure-distance comparisons from existing data on model and large-scale detonations in underground magazines.....	27
13. Airblast Inhabited Building Distance versus total loading density for selected model and large-scale tests.....	28
14. Photos of debris fields from Brick Model Tests.....	29
15. Ejecta distribution as a function of azimuth along the 6.2 m arc; Brick Model Test 3.....	30
16. Launch velocities of cover rock ejecta.....	31
17. Comparison of relative debris densities from Brick Model Test 3 with the Shallow Underground Tunnel/Chamber Explosion Test	32

LIST OF FIGURES (Cont'd)

<u>Figure No.</u>		<u>Page</u>
A1-A7	Brick Model Test 1: Airblast gage records.....	41-47
A8	Brick Model Test 1: Accelerometer record.....	48
B1-B10	Brick Model Test 2: Airblast gage records.....	50-59
B11-B14	Brick Model Test 2: Acceleration and velocity records.....	60-63
C1-C8	Brick Model Test 3: Airblast gage records.....	65-72

LIST OF TABLES

<u>Table</u> <u>No.</u>		<u>Page</u>
1.	Brick Model Tests: Measurement Type and Gage Location Data.....	33
2.	Brick Model Tests: Explosives Charges and Chamber Cover Thicknesses.....	33
3.	Brick Model Test 1: Airblast Pressure and Ground Shock Measurements	34
4.	Brick Model Test 2: Airblast Pressure and Ground Shock Measurements.....	35
5.	Brick Model Test 3: Airblast Pressure and Ground Shock Measurements.....	36
6.	Effects of Magazine Cover Resistance on Airblast.....	37
7.	Brick Model Test 3: Brick Ejecta Distributions.....	38

CONVERSION FACTORS, METRIC (SI) TO NON-SI
UNITS OF MEASUREMENT

SI (Metric) units of measurement used in this report can be converted to Non-SI units as follows:

Divide	By	To Obtain
cubic metres	0.02831685	cubic feet
kilograms	0.4535924	pounds (mass)
kilograms per cubic metre	16.01846	pound (mass) per cubic foot
kilopascals	100.	bars
kilopascals	6.894757	pounds (force) per square inch*
metres	0.3048006	feet
metres per kilogram ^{1/3}	0.3955977	feet per pound ^{1/3}
milliseconds	1000.	seconds
radians	0.1745329	degrees (angle)
square metres	0.09290304	square feet

* For pressure, 14.7 psi = 1.0 atmosphere = 1.014 bar = 101.4 kPa

BRICK MODEL TESTS OF
SHALLOW UNDERGROUND MAGAZINES

SECTION 1

INTRODUCTION

1.1 BACKGROUND

A considerable amount of research has been performed in the last two decades to develop data and prediction methods for airblast and debris hazards from accidental explosions in underground magazines. Much of this work is concerned with detonations in magazines so deep that venting does not occur. The effect of cover venting on reduction of external airblast was initially investigated in small-scale tests (1:25) performed in the United Kingdom (Millington, 1985). More recently, the Shallow Underground Tunnel/Chamber Explosion Test (Joachim, 1990), sponsored by the KLOTZ Club*, provided full-scale airblast and debris/ejecta data for a shallow underground magazine containing 20,000 kg**, net explosive weight (NEW).

In 1980, the U.S. Army Engineer Waterways Experiment Station (WES) conducted a series of intermediate-scale (500-kg charges) cratering tests in open shafts in rock for the Federal Republic of Germany (Davis, 1981). The results showed a definite effect of rock strength and structure (jointing) and terrain surface slope, as well as the charge cover depth, on the size and shape of the crater produced, and on the amount, direction, and velocity of ejecta thrown out. Earlier 1:75-scale model tests by WES (Joachim, 1988 and Smith, 1989) of fully contained detonations in long chambers in rock showed that formulae for predicting strain and spall velocities in adjacent chambers must include, as a minimum, a characteristic modulus value for the rock surrounding the chamber.

* The KLOTZ Club is an ad hoc committee, representing the defense agencies of France, Germany, Norway, Sweden, Switzerland, the United Kingdom, and the United States, which sponsors research to improve the safety of ammunition storage.

** A table of factors for converting SI units of measurement to Non-SI units is presented on page vi.

These results strongly imply that, at large scales where extensive volumes of rock must be moved during the venting process, the gross (as opposed to unit) strength and structure of shallow rock covers may be important factors in predicting the extent of rupture of the cover, and the ejecta hazard ranges, from site to site. This is in addition to the known problem of accounting for the variations in cover thickness and surface slope.

The 1988 Shallow Underground Test provided data for a single site, consisting of a weak, highly jointed rock. In actual practice, however, magazines of this design have been constructed at sites having a wide range of rock strengths and cover thicknesses over the magazine chamber. In addition, the loading densities of the magazines differ from site to site. To investigate the influence that these variations would have on the external blast hazards from an accidental explosion, and the extent that their effect can be reproduced in small-scale tests, a series of model tests were conducted in this study to provide a comparative basis to evaluate these factors. In particular, it was desired to compare the external airblast (beyond the tunnel portal) with that measured in previous model tests which simulated solid rock or soil (sand) covers, as well as the airblast measured in the large-scale 1988 Shallow Underground Test.

1.2 OBJECTIVE

The overall objective of the Brick Model test program was to determine the hazardous effects (airblast and debris) produced by an accidental detonation of explosive stores which ruptures the overhead cover of an underground magazine. Specific test objectives were to evaluate the effects of explosive loading density (kg of explosive per m³ of chamber volume) and the thickness and strength of the rock cover on the external blast hazards, and the ability of small-scale models to reproduce large-scale test results.

SECTION 2

PROCEDURES

2.1 APPROACH

Models of underground munitions storage magazines were constructed at 1:25 scale and tested to evaluate the effect of cover depth, cover structure/strength, and loading density on ejecta throwout and venting relief of the access tunnel airblast pressures. The basic model consisted of a single storage chamber and access tunnel constructed in a large testbed of paving brick, simulating a jointed rock mass. The dimensions of the storage chamber and access tunnel corresponded to a 1:25-scale model of those constructed for the 1988 Shallow Underground Tunnel/Chamber Explosion Test. The model access tunnel was 1.0 m long with a cross-sectional area of 84.4 cm² (9.6 cm in height and width; see Figure 1). The model storage chamber was 72 cm long, with a cross-sectional area of 294.4 cm² (20 cm wide by 16 cm high; see Figure 2).

Dynamic measurements included: (1) chamber pressures, (2) access tunnel pressures, (3) external airblast pressures, and (4) motion (acceleration) of the simulated rock mass above the chamber. The airblast and ground motion gage locations are shown in Figure 3 and listed in Table 1. Passive measurements consisted of post-test surveys of debris distributions for Test 3, and observations of the extent of cover rupture and debris throw on all three tests.

2.2 MODEL CONSTRUCTION

All models were constructed with solid paving bricks (without mortar) inside a reinforced concrete containment structure, as illustrated in Figure 4. Nominal dimensions of the bricks were 5.8 by 9.3 by 19.7 cm. As shown in Figure 4, the bricks were laid with the wide face (9.3 by 19.7 cm) in the vertical plane, and with the long axis rotated 30° from the vertical, in the direction of the portal. Thus, the overburden surface slope of the models was 30 degrees. A thin layer of sand was placed over the surface of the bricks to simulate soil overburden.

The chamber and access tunnel were formed around galvanized steel sheet metal, shaped to the required cross-sections (Figures 1 and 2). A layer of mortar approximately 4 cm thick was placed around the top and sides of the chamber form to fill voids between the form and the bricks, and bricks were placed around the assembly. The same procedure was used to form the access tunnel in the model. The chamber was constructed first, and the sheet metal form removed prior to installation of the tunnel section. Figure 5 compares a front view of the completed model (for Test 1) with a similar view of the large-scale Shallow Underground Test magazine.

2.3 INSTRUMENTATION

Two accelerometers were positioned in the overburden above the tunnel/chamber centerline to measure the motions of the cover material for each test. Selection of accelerometer gage ranges was based on an extrapolation of ground shock data from the large-scale Shallow Underground Test. The accelerometers were mounted in small, WES-designed, two-part cylindrical canisters. Each gage canister consisted of an outer cylinder with a tapered, truncated, conical inner surface, and a matching insert with a flat center section milled parallel to the axis. The gage was mounted on this flat section before the tapered plug was inserted into the outer cylinder. The canister was cemented into a hole drilled in a solid brick, which was placed at the desired gage location in the model. The canisters were oriented to measure motion perpendicular to the surface slope of the model. Cables were placed in 6.4-mm-diameter stainless steel tubing, which was routed away from the chamber.

Four internal airblast pressure gages were installed for each test--two gages in the chamber wall and two in the access tunnel floor--to record the internal pressure environment. The gages were mounted in metal fixtures inserted into 1.9-mm-diameter PVC pipe. The pipes were routed between the bricks to the side and rear of the test bed. The voids around the PVC pipes were packed with masonry sand to minimize the density discontinuity.

Six free-field pressure gages were permanently installed in front of the tunnel portal, along the extended tunnel/chamber centerline. The gage mounts were cast into a 10-cm thick concrete slab. The concrete slab was 1.8 m wide

and extended a distance of 6 m from the tunnel portal. The surface of the pavement was level out to a distance of 1.5 m, where a downward slope (11 degrees) began.

One total (stagnation) pressure measurement was attempted outside the tunnel at a distance of 20 cm from the portal. A probe fashioned from 6.4-mm diameter stainless steel tubing was attached to a gage mount cast into the concrete slab. The entrance of the tube was positioned 2.5 cm above the surface-mounted, side-on overpressure gage located 20 cm from the access tunnel portal.

The gage signals were amplified, digitized and recorded on computer-controlled, transient data recorders. The gage signals were transmitted to the recording trailer on 4-conductor, shielded cable (approximately 200 m long) with a floating ground. Each channel was electrically calibrated at the digitizer by the equivalent voltage method.

2.4 EXPLOSIVE CHARGES

The explosive charges were assembled from 0.085-kg/m (400-grain per foot) PETN detonating cord, cut in 48-cm lengths. The detonating cord was bundled around and taped to a thin wood slat, which was pushed through the access tunnel into the chamber (Figure 6). The slat was just long enough to be contained completely within the chamber (approximately 72 cm). The explosive charge was approximately 5 cm in diameter for Tests 1 and 3, and 1.3 cm for Test 2. All charges were initiated from the portal end using a Reynolds Industry exploding bridge wire (EBW) detonator (Model RP-83). Charge weights, chamber loading densities, and dimensions of the explosive charges are given in Table 2.

2.5 EJECTA/DEBRIS COLLECTION

Both previous test experience and analytical studies have clearly shown that, while debris throw ranges and relative distributions can be scaled by model tests, the areal density (impacts per m^2) cannot. This is because the model material which comprises the debris source does not break up with the same size distribution as does the prototype material. Consequently, for Tests 1 and 2, only the maximum range of ejecta/debris was recorded. However, a more detailed ejecta survey was made after Test 3. The boundary of each sample area was marked on the ground using a square frame covering an area of $1 m^2$. The location of the sample areas are shown in Figure 7. During sampling, the frame was centered at the required distance and azimuth and the number of pieces of brick, either whole or broken, within the frame area was counted. The distribution data was broken down into the number of pieces smaller than half of a brick, and those larger than half.

SECTION 3

RESULTS AND DISCUSSION

3.1 AIRBLAST EFFECTS

3.1.1 Comparisons of Model and Large-Scale Test Results. The airblast arrival times, peak pressures, and peak impulse values (from integration of the time histories) obtained on the Brick Model Tests are given in Tables 3, 4, and 5. Scaled arrival time data are plotted versus scaled distance from the initiation ends of the explosive charges in Figure 8. A comparison is shown with the airblast arrival times measured on the Shallow Underground Test. There is excellent agreement between the model and prototype measurements for the external gages. The arrival times for the gages inside the model tunnel are slightly lower (i.e., faster) than occurred inside the prototype tunnel.

The prediction curves for airblast peak pressure (external) originally developed for the large-scale Shallow Underground Test are presented in Figure 9. The Shallow Underground Test and the corresponding model (Test 1) data are included for comparison. The distances from the model portal were multiplied by the 1:25 scale factor in this plot to match the prototype scale. As shown here, the model data clearly falls within the band spread of the predictions.

3.1.2 External Airblast Attenuation - Comparison with Previous Experiments. In Figure 10, the ratio of calculated exit pressure to measured free-field overpressure is plotted versus normalized distance from the tunnel portal for all available data from previous tests of underground magazines. The Brick Model Tests (WES Model (1:25)) are included, along with six other model series, and two full-scale tests, including the Shallow Underground Test (KLOTZ (88)). The exit pressures were calculated from the relation given by Vretblad, 1988:

$$P_w = 17.7 (Q / V_T)^{0.45}$$

where P_w is the exit pressure, bars

Q is the TNT-equivalent explosive weight, kg

and V_T is the total volume of the underground facility, m^3 .

A reference line through the data in Figure 10 can be expressed by the equation

$$P_w / P_{so} = 1.0 (R / D)^{1.35}$$

and $D = 4 A / p$

where P_{so} is the free-field overpressure, bars

R is the horizontal distance from the portal, m

D is the hydraulic diameter of the tunnel (for turbulent flow), m

A is the minimum cross-sectional area of the tunnel, m²

and p is the perimeter of the minimum cross-sectional area, m

As shown in Figure 10, the data exhibits considerable scatter, with many of the points lying above the reference line. Note however, that the results of both the Brick Model tests and the Shallow Underground Test (solid data points) fall well within the scatter band, near the reference line.

3.1.3 Effect of Cover Strength and Thickness. Table 6 lists the Inhabited Building Distances (scaled up to full-scale ranges) derived from five model tests with similar loading densities, but different scaled cover depths and cover material strengths. There is a clear trend in the effect of the overall integrity of the chamber cover on the IBD. With similar cover thicknesses and loading densities, the heavily-jointed brick model produced about the same long-range blast pressures as did the Norwegian sand model. Based on the IBD's, however, the Norwegian concrete model produced a long-range blast pressure equivalent to a heavily-jointed brick model with almost twice the cover thickness.

Measured peak pressures from all three Brick Model tests are plotted in Figure 11. The DDESB airblast prediction equation and the curve fit to the peak overpressure data of the Shallow Underground Test are included in Figure 11 for comparison. Although there is some data scatter, certain trends are indicated. When the cover depth was held constant and the loading density was reduced from 60 to 10 kg/m³ (Test 2 versus Test 1), the portal pressure was reduced by a factor of about four, and the long-range external pressures were about halved. When the scaled cover depth of the brick models was increased

from 0.44 to 0.79 m/kg^{1/3} (Test 3 versus Test 1), and the chamber loading density held constant at 60 kg/m³, the side-on overpressures outside the tunnel portal increased an average of 30 percent. The peak pressure midway down the access tunnel increased by about 130 percent. When the scaled cover depth was held constant at 0.8 m/kg^{1/3}, an increase in chamber loading density from 10 to 60 kg/m³ (Test 3 versus Test 2) produced an average of 250 percent increase in the free-field side-on overpressure outside the portal.

From Figure 11, it is interesting to note the degree to which the internal and external airblast overpressures measured on the large-scale, Shallow Underground Test were reproduced in the 1:25-scale brick model (Test 1). In general, the model provided a good representation of the prototype results. The tunnel exit pressures match very closely, but external overpressures were low by a factor of approximately three in the free-field. However, these lower pressures may have been due to the downward slope of the ground surface constructed for the model (see Figure 3) at the far-field gage stations.

The peak impulse values from the model tests, obtained by integrating the overpressure-time histories, are plotted versus distance from the charge initiation point in Figure 12. The peak impulse data curve from the Shallow Underground Test are included in Figure 12 for comparison. Although peak impulse shows more scatter than the overpressure data, the model and prototype data clearly follow the same trends.

3.1.4 Responding Versus Non-Responding Magazines. Figure 13 is a plot of Inhabited Building Distance (distance to the 5.0 kPa pressure level) versus loading density for selected tests, where the loading density is based on the total volume of the storage facility (i.e., the volume of the chamber plus the access tunnel). A curved line has been drawn through the data points for the WES 1:75-scale model test (Smith, et al, 1989). These small-scale tests were conducted in a model chamber and access tunnel constructed from steel pipe. Therefore, this model represents a totally non-responding magazine structure. The data from the large-scale 1987 KLOTZ test at Alvdalen, Sweden (Vretblad 1988) fall very close to the WES 1:75-scale model curve. The Alvdalen tests were conducted in rock chambers with sufficient overburden to prevent rupture and cover venting, and therefore also represent non-responding structures.

The remaining data presented in Figure 13 are from tests where the overburden ruptured (responding magazines), allowing release of the detonation gas pressures in the storage chamber through the cover venting. The full-scale Inhabited Building Distances (IBD's) derived from the Shallow Underground Test, the Brick Model Tests, and the Norwegian model tests (Jenssen and Krest, 1988) all fall well below the IBD curve for the non-responding magazine tests, by about a factor of four.

While the IBD's for the responding magazines may at first appear unrelated, certain trends are indicated. For example, the Brick Model Tests show an increase in IBD of 25 percent (from 212 to 266 m in full-scale) when the scaled cover thickness was increased from 0.44 to 0.79 m/kg^{1/3}. Similarly, increasing the total loading density (mass of explosives divided by total volume of the underground facility) from 7.1 to 42.9 kg/m³ increased the IBD by 77 percent (from 150 to 266 m), when the scaled cover depth was held constant at about 0.8 m/kg^{1/3}.

3.2 DEBRIS EFFECTS

3.2.1 Debris Launch Velocities. Successful measurements of the cover accelerations for the Brick Model Tests were obtained only on Test 2, which had the lowest loading density. A partial record was obtained for one of the two accelerometers (EM-1) installed for Test 1, but the peaks of the acceleration wave form were clipped due to over-ranging of the gage. The wave form was clipped at 6,000 g's, and the portion recorded indicated that the actual peak might have been close to 10,000 g's. No useful records were obtained from the accelerometers on Test 3.

Assuming that the bricks just below the slope surface above the chamber were launched in an initial direction normal to the surface, a launch velocity can be roughly calculated based on the measured throw distance. This calculation indicates a launch velocity of about 4.9 m/sec for Test 1.

The acceleration wave forms obtained for Gages GM-1 and GM-2 on Test 2 (see Figure B.11 and B.13 in Appendix B) showed severe "ringing" of the gages, possibly due to shock reverberations in the bricks containing the gages. It

was possible, however, to integrate these acceleration records to obtain velocity and displacement histories. As shown in Figure B.12, the gage located 18.3 cm above the model chamber roof experienced a peak velocity of only 1.1 m/sec, and a total displacement of about 0.5 mm. Because of the large scaled cover thickness for this test ($0.80 \text{ m/kg}^{1/3}$), the cover material at this small distance above the chamber was not moved significantly by the late-time gage pressures, but experienced only a small displacement as the initial shock wave passed through it on its way to the surface. Gage GM-2, located about mid-depth in the cover, experienced a similar peak acceleration. Because it was nearer to the free surface than Gage GM-1, however, it moved at a somewhat higher peak velocity (2.0 m/sec) and was displaced a greater distance. The velocities and displacements of the brick layers increased dramatically with proximity to the cover surface. The bricks at the top of the chamber cover spalled completely free, but still with insufficient velocity to constitute long-range debris.

3.2.2 Debris Distribution. The maximum ranges of debris observed on the Brick Model Tests were 91 m for Test 1, and 32 m for Test 3. Using $W^{1/6}$ scaling, the range for Test 1 is less than half the maximum range observed on the large-scale test. On Test 3, the explosive charge was larger than that of Test 2, but the cover thickness was also greater, resulting in the same (or nearly so) scaled cover thickness of $0.8 \text{ m/kg}^{1/3}$. As shown in the photos of Figure 14, the upper layers of brick again spalled away from their in situ positions, traveling to significantly greater distances than occurred for Test 2. Table 7 gives the surveyed distribution of debris from Test 3. All of the debris moved outward from the surface slope over the tunnel and chamber, within a sector extending about 30 degrees to each side of the extended tunnel axis (see Figure 15). The vast majority of debris pieces were fragments less than 1/2 brick in size, indicating that the initial shock shattered most of the bricks near the surface.

3.2.3 Comparisons with Previous Tests. Figure 16 shows a series of curves (from Helseth, 1982) relating debris launch velocity to the scaled cover thickness and the magazine loading density. The data sources range from aircraft shelters, which had very shallow cover thicknesses and loading densities, to buried cratering charges, which had very deep covers and very

high loading densities. Underground magazines would typically fall between two extremes.

Dimensional analyses show that the ratio of velocities measured in a model test to those occurring in a full-scale test is equal to the square root of the model scale factor. Therefore, the peak velocity measured by Gage GM-2 in Test 2 of the Brick Model Tests was multiplied by 5, and plotted in Figure 16 along with launch velocities recorded on the large-scale Shallow Underground Test. While this single data point from the Brick Model Tests appear to almost exactly match the curves and other data of Figure 16, it must be remembered that the Gage GM-2 was not at the cover surface, but at mid-depth in the cover. The actual launch velocity for Test 2 (small though it was, as evidenced by the short debris travel) was no doubt somewhat greater than at the gage point.

Also shown in Figure 16 is the launch velocity based on the ballistic calculation for Test 1 (see Section 3.2.1). The value, which was also multiplied by a velocity scaling factor of 5 for plotting on Figure 16, appears to be somewhat low in comparison to the full-scale Shallow Underground Test.

Figure 17 shows the debris areal density (number of impacts per square metre), as a function of range from the tunnel portal, for Brick Model Test 3 compared to that of the large-scale Shallow Underground Test. In accordance with accepted scaling procedures for ejecta/debris (Rooke, 1980), the distances in the model case have been scaled up by multiplying by the sixth root of the ratio of the model-versus-prototype charge weights, i.e., $(20,000 \text{ kg}/1.27 \text{ kg})^{1/6}$.

As stated earlier in Section 2.5, however, it is not possible to quantitatively compare the debris densities of the Brick Model Tests with those of the full-scale test, since the number of fragments produced by the cover breakup does not scale. Therefore Figure 17 should be regarded only as a comparison of the relative debris densities recorded on Brick Model Test 3 as a function of range and azimuth, with similar relations from the large-scale test. To provide such a comparison, the entire grouping of the model data has been arbitrarily positioned with respect to the ordinate scale of Figure 17. Considering this limitation, the comparison is actually quite

good. the attenuation of the model impact densities with distance closely matches the shape of the curves from the large-scale data. The relative differences between the debris densities along the extended tunnel axis (0-degree azimuth) and the densities "off-axis" also compare quite well with the large-scale results.

SECTION 4

CONCLUSIONS AND RECOMMENDATIONS

4.1 CONCLUSIONS

Peak airblast overpressure and impulse values measured on the Brick Model Tests at the tunnel exit and in the near-field (just outside the portal) closely match the results of the corresponding large-scale test. The model pressure data in the far-field was somewhat lower than measured in the large-scale test, possibly due to the gravity and inertial effects resulting from our inability to properly scale the overburden. A comparison among the model test results shows an increase in pressure of a factor of 4 to 6 when the chamber loading density was increased from 10 to 60 kg/m³. An overpressure increase on the order of 90 percent was seen when the scaled overburden thickness was increased from 0.44 to 0.79 m/kg^{1/3}. The Inhabited Building Distances indicated by the model tests were significantly less than those found for the large-scale Shallow Underground Test, but this was also attributed to overburden scaling deficiencies.

Ejecta impact data collected from Brick Model Test 3 demonstrate the feasibility of modeling the basic nature of overburden ejecta throwout. Because the breakup of the cover material does not scale, however, ejecta sizes in the model tests were much too large to accurately define the ejecta hazard range, in terms of impacts-per-square meter.

4.2 RECOMMENDATIONS

The results of the tests conducted in this study demonstrate that some explosion effects can be very accurately simulated in small-scale models, while others are biased by properties of the test environment that are not normally scaled with sufficient accuracy. For example, the peak internal airblast pressures in the brick model closely matched the full-scale China Lake Test. The external pressures, however, were lower in the Brick Model Test than in the full-scale event, apparently due to an earlier venting of the long-duration chamber pressures in the model. This, in turn, was probably due to the fact that the mass of the cover material, which resists the venting force, cannot be properly scaled in a normal "lg" model. For the same reason,

it is not possible to accurately simulate the breakup of the cover rock in such a model, nor the range to which the debris is thrown.

It is strongly recommended that, before further model tests of responding magazines are conducted, a thorough analysis be made of the fundamental physics of the explosion/response problem for responding magazines in order to clearly identify the inter-relationships between the model/prototype properties and the outcome parameters. Two approaches for such an analysis are recommended. The most inexpensive would be the development of a single computer model which idealizes the problem, and predicts outcomes based on simple physical laws. A more revealing approach involves the use of numerical computer codes capable of treating a structure "breakup." Some of the recently-developed versions of the Discrete Element Code are ideally suited to such a problem. These codes have been used previously to study the formation and throw velocities of debris from simple cratering explosions in jointed rock, and have provided significant insights into the actual influence of factors such as rock strength and density, joint patterns and shear strengths, and overburden surface slopes.

REFERENCES

1. Davis, Landon K.; and McAneny, Colin C.; 1981, "Project SPERRE, Report 5, Summary Report: Road Cratering Tests in Rock With Preemplaced Charges," Technical Report SL-81-5, U.S Army Engineer Waterways Experiment Station, Vicksburg, MS.
2. Helseth, Einar S.; "Underground Ammunition Storage, Model test in scale 1:100 in Sand," Fortifikatorisk Notat NR 160/82, Progress Report to KLOTZ Club Meeting, Norfolk, VA.
3. Jenssen, Arnfinn; and Krest, Ottar; 1988, "Shallow Underground Ammunition Magazine Trials at Naval Weapons Center (NWC), China Lake, Ad Hoc Model Tests, Approximate Scale 1:24.8," FORTIFIKATORISK NOTAT NR 192/88, Norwegian Defence Construction Service, Oslo Norway.
4. Joachim, Charles E.; and Smith, Dennis R.; 1988, "WES Underground Magazine Model Test," Twenty Third DOD Explosives Safety Seminar, Atlanta, GA.
5. Joachim, Charles E.; 1990, "Shallow Underground Tunnel/Chamber Explosion Test Program, Summary Report," Technical Report SL-90-10, U. S. Army Engineer Waterways Experiment Station, Vicksburg, MS.
6. Millington, Charles, 1985, "The Ernestettle Report," Preliminary AWRE Report UK(ST)IWP 205, 0/1/85, AWRE (Foulness), Ministry of Defence, United Kingdom.
7. Rooke, Allen D., Jr., 1980, "Crater-Ejecta Hazard Predictions in Cohesive Soils, The Middle Gust 1 Event," Thesis, Master of Science, Mississippi State University, Mississippi State, MS.
8. Smith, Dennis R.; Joachim, Charles E.; Davis, Landon K.; and McMahon, Gordon W.; 1989, "Effects of Explosions in Underground Magazines," Technical Report SL-89-15, U.S. Army Engineer Waterways Experiment Station, Vicksburg, MS.
9. Stromsoe, E.; 1969, "Underground Explosion Trials at Raufoss 1969, Measurement of Airblast Outside The Tunnel," Intern Rapport X-124, FORSVARETS FORSKNINGSINSTITUTT, Norwegian Defence Research Establishment, Kjeller, Norway.
10. Vretblad, Bengt; 1988, "Data from the 1987 KLOTZ Club Tests In Sweden, Report C3:88, FORTIFIKATIONSFORVALTNINGEN, FORSKNINGSBYRAN, Eskiltuna, Sweden.

Area = 84.8 cm²

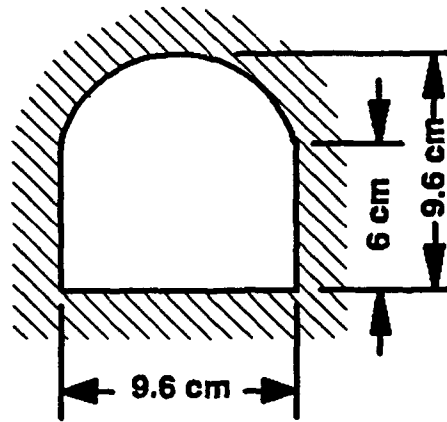


Figure 1. Access tunnel cross-section for 1:25-scale WES Brick Model Tests

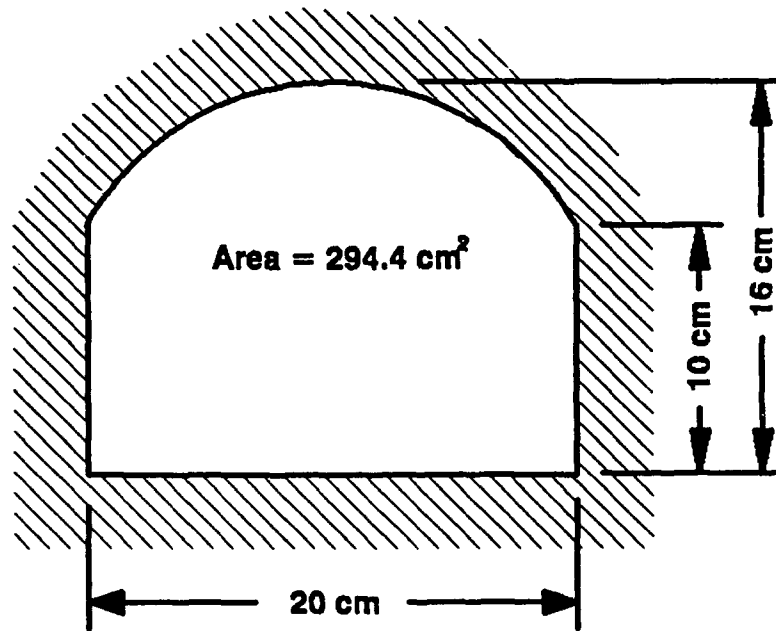


Figure 2. Storage chamber cross-section for 1:25-scale WES Brick Model Tests.

LAYOUT OF MODEL PROFILE ALONG CENTERLINE

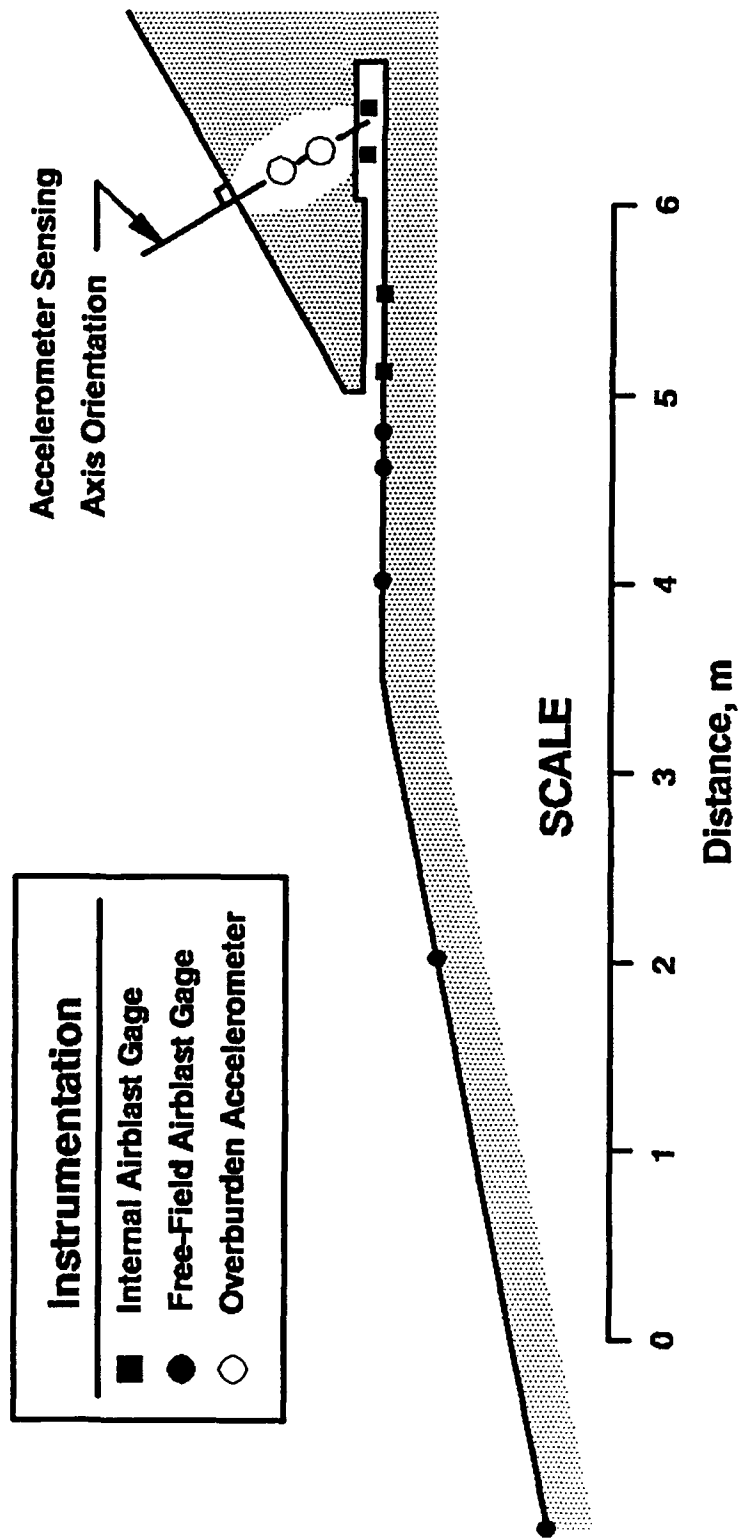


Figure 3. Layout (centerline profile) of 1:25-scale WES Brick Model.

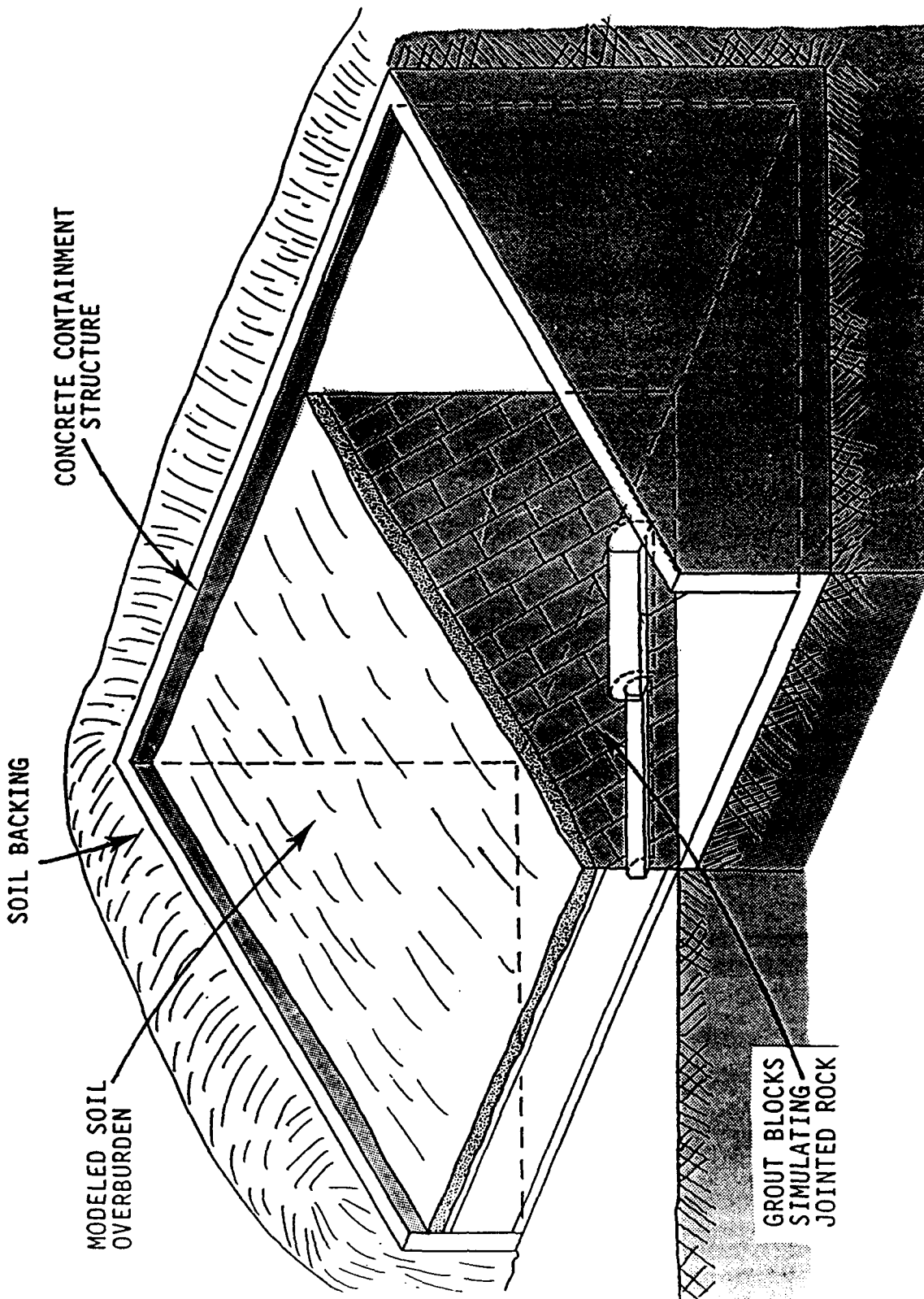
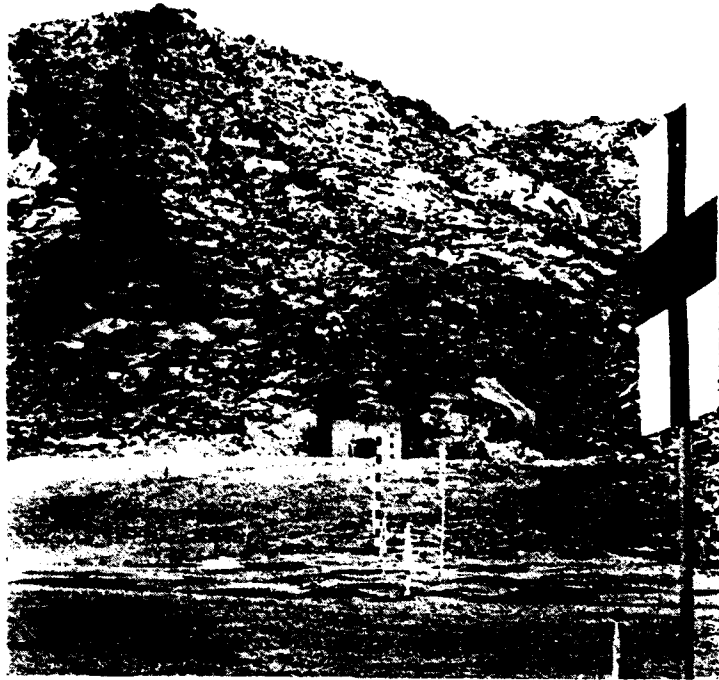


Figure 4. Testbed design for 1:25 scale tests of influence of cover rock characteristics on venting, ejecta, and internal/external airblast levels for shallow underground magazines.



a. Large-scale Shallow Underground Test.



b. Brick Model Test 1.

Figure 5. Tunnel portals and foreground areas (for external external airblast measurements) of the large-scale Shallow Underground Test and the corresponding Brick Model Test.

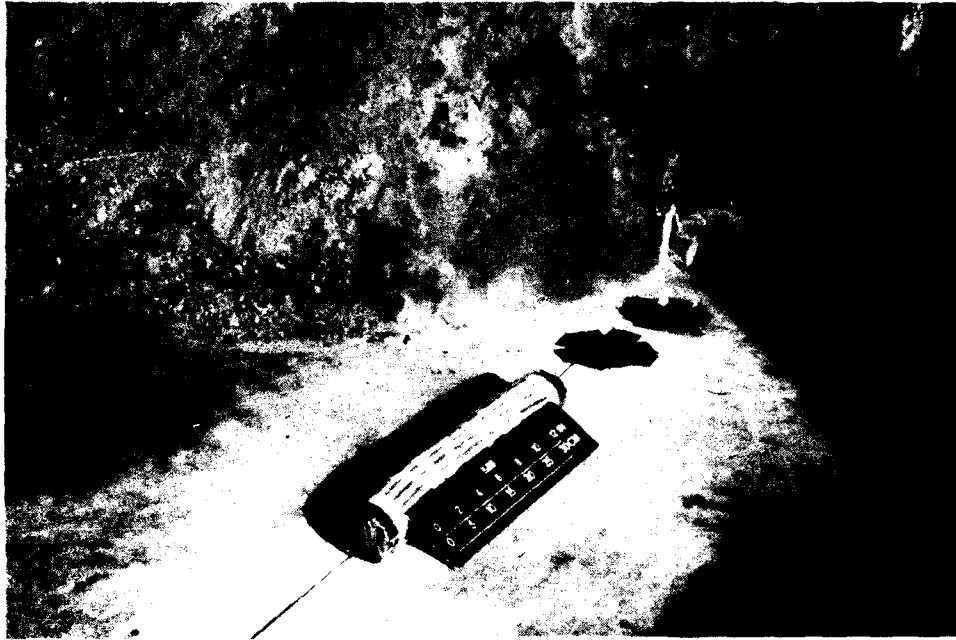


Figure 6. 1.27-kg explosive charge before insertion into chamber of Brick Model Test.

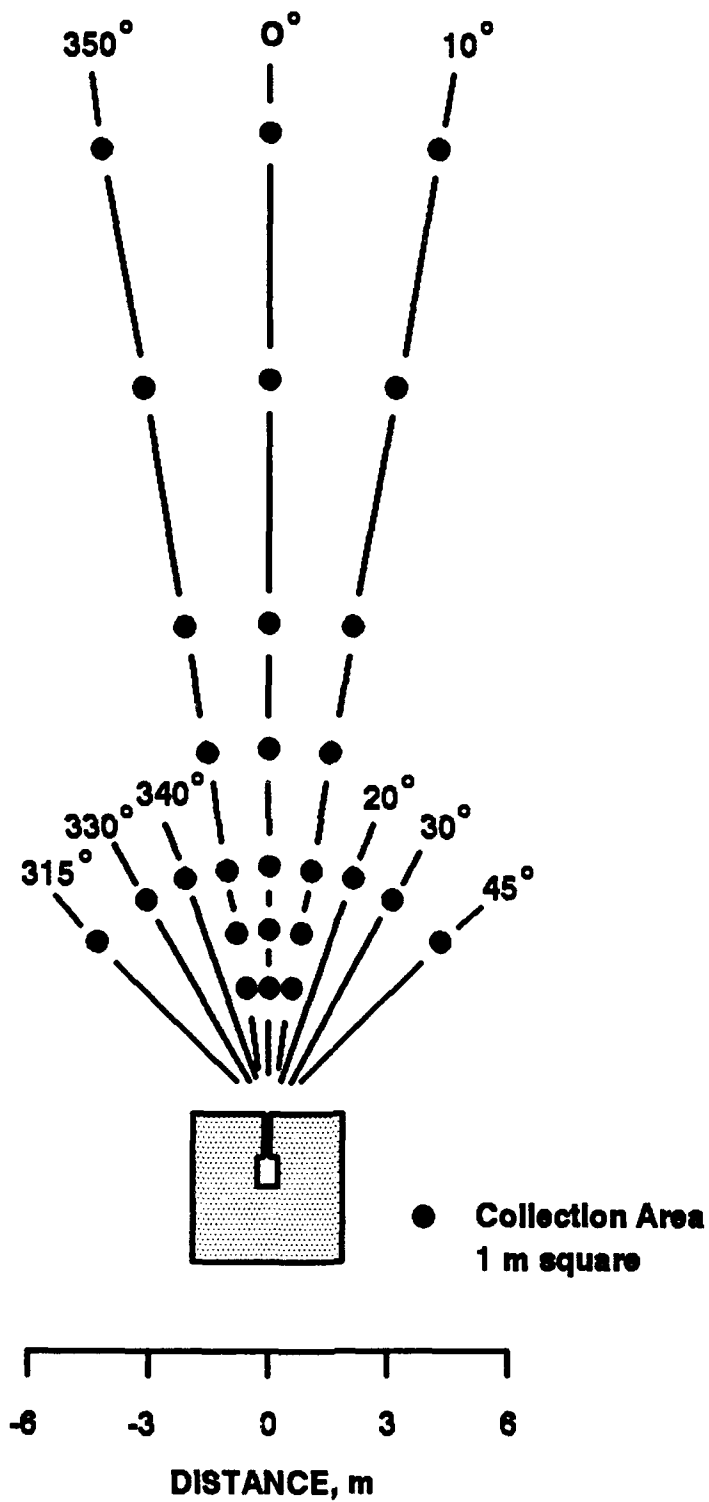


Figure 7. WES Brick Model Test 3: location of ejecta collection areas.

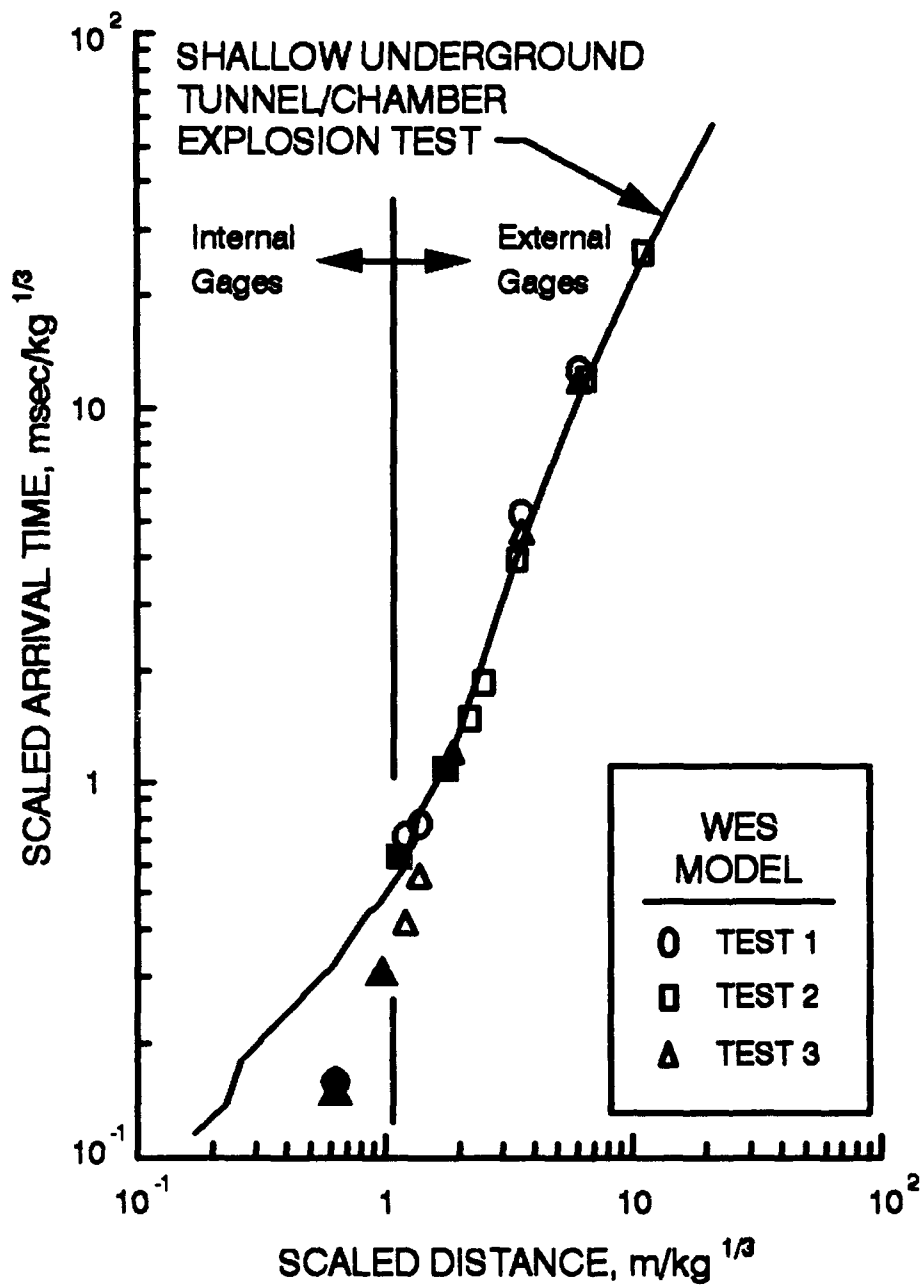


Figure 8. Scaled arrival time versus scaled horizontal distance from the charge initiation point. A comparison is shown between the prototype (Shallow Underground Tunnel/Chamber Explosion Test, loading density 60 kg/m³) and the Brick Model Test data. Solid symbols are internal gages in the model tests.

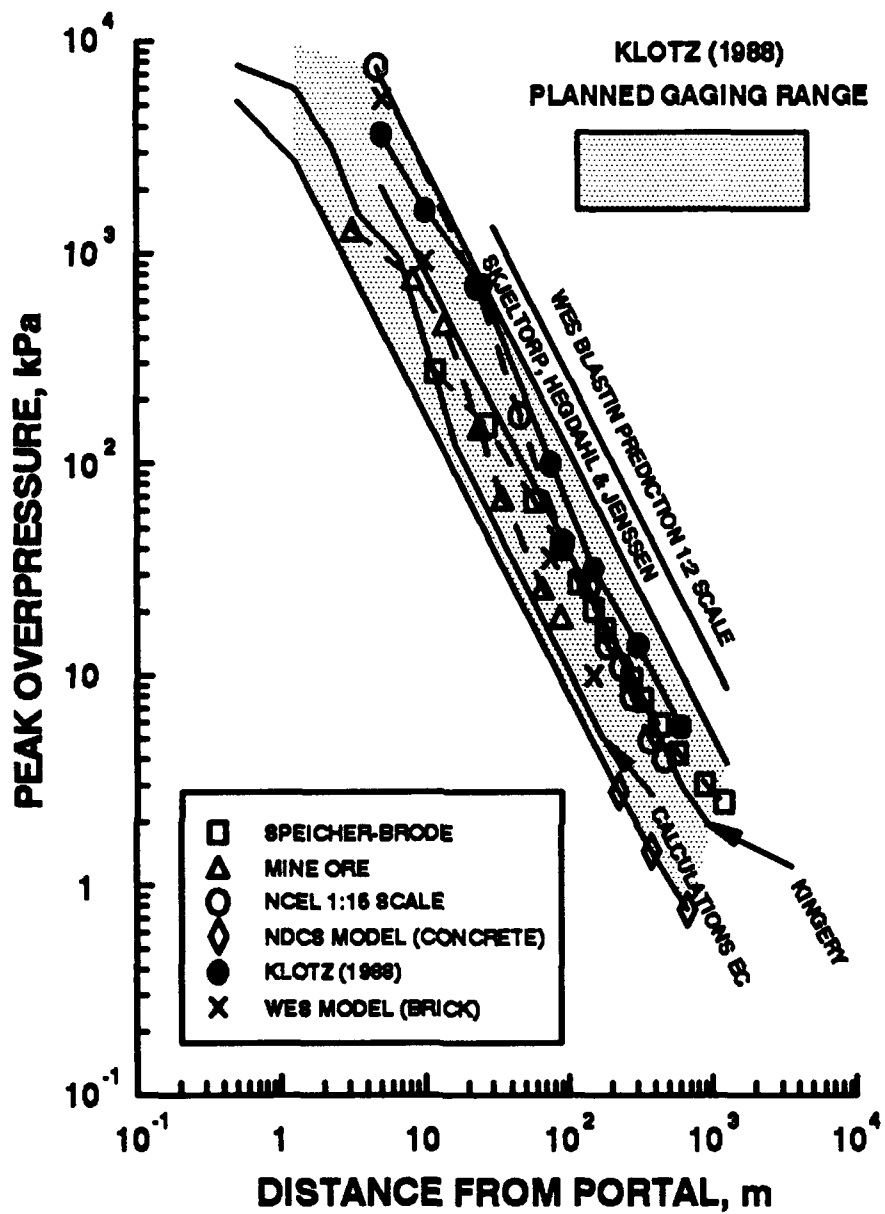


Figure 9. Free-field side-on overpressure scaled to the Shallow Underground Tunnel/Chamber Explosion Test (KLOTZ 1988) parameters.

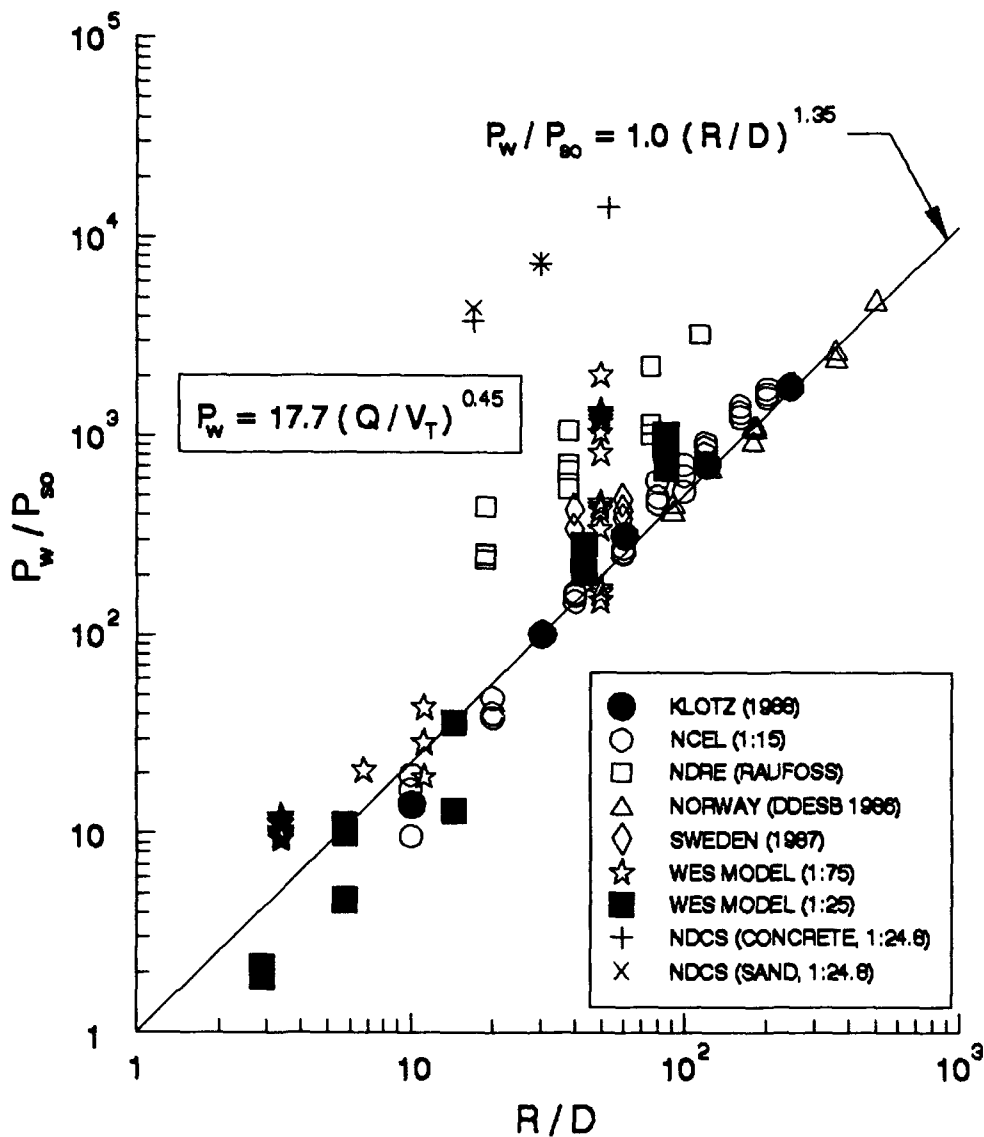


Figure 10. Pressure-distance comparisons from existing data on model and large-scale detonations in underground magazines. The ratio of calculated exit pressure (P_w) to measured free-field side-on overpressure (P_∞) is plotted versus distance (R) from the tunnel portal along the tunnel/chamber centerline. The distance is normalized by dividing by the hydraulic diameter (for turbulent flow) of the access tunnel cross-section.

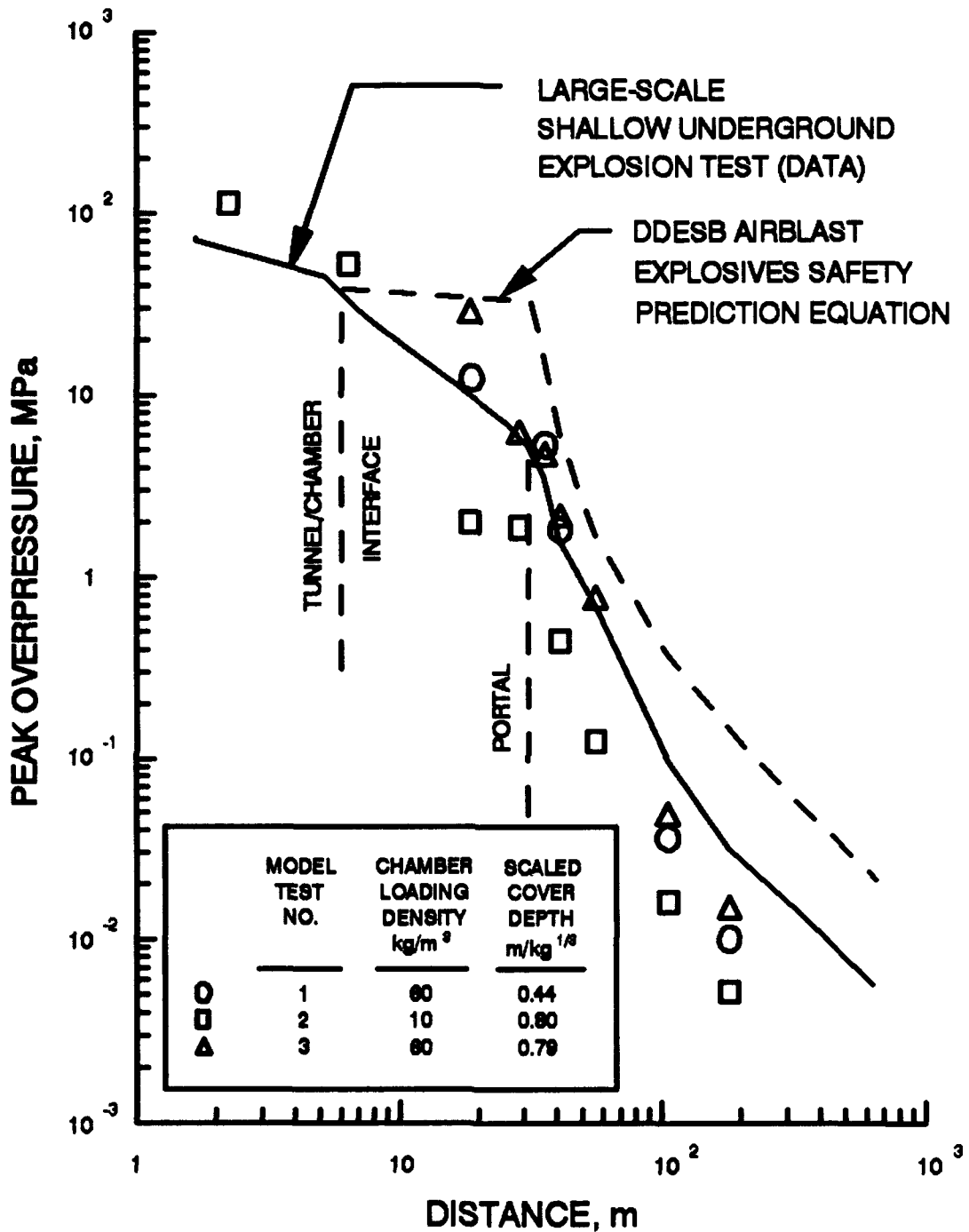


Figure 11. Peak side-on overpressure versus horizontal distance from the charge initiation point. A comparison is shown between the prototype (Shallow Underground Tunnel/Chamber Explosion Test, loading density 60 kg/m³) and the WES Brick Model Test data.

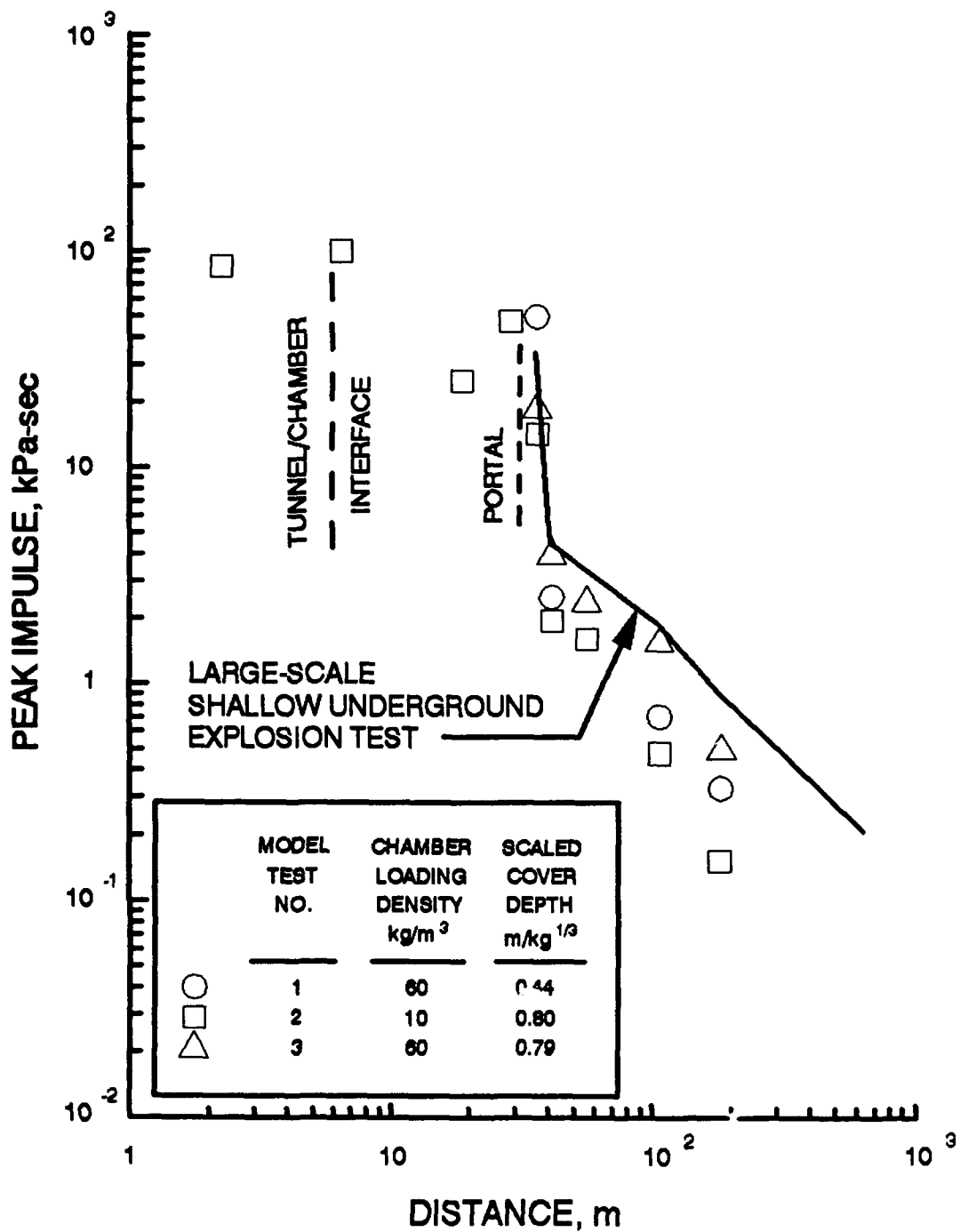


Figure 12. Peak side-on impulse versus horizontal distance from the charge initiation point. A comparison is shown between the prototype (Shallow Underground Tunnel/Chamber Explosion Test) and the WES Brick Model Test data.

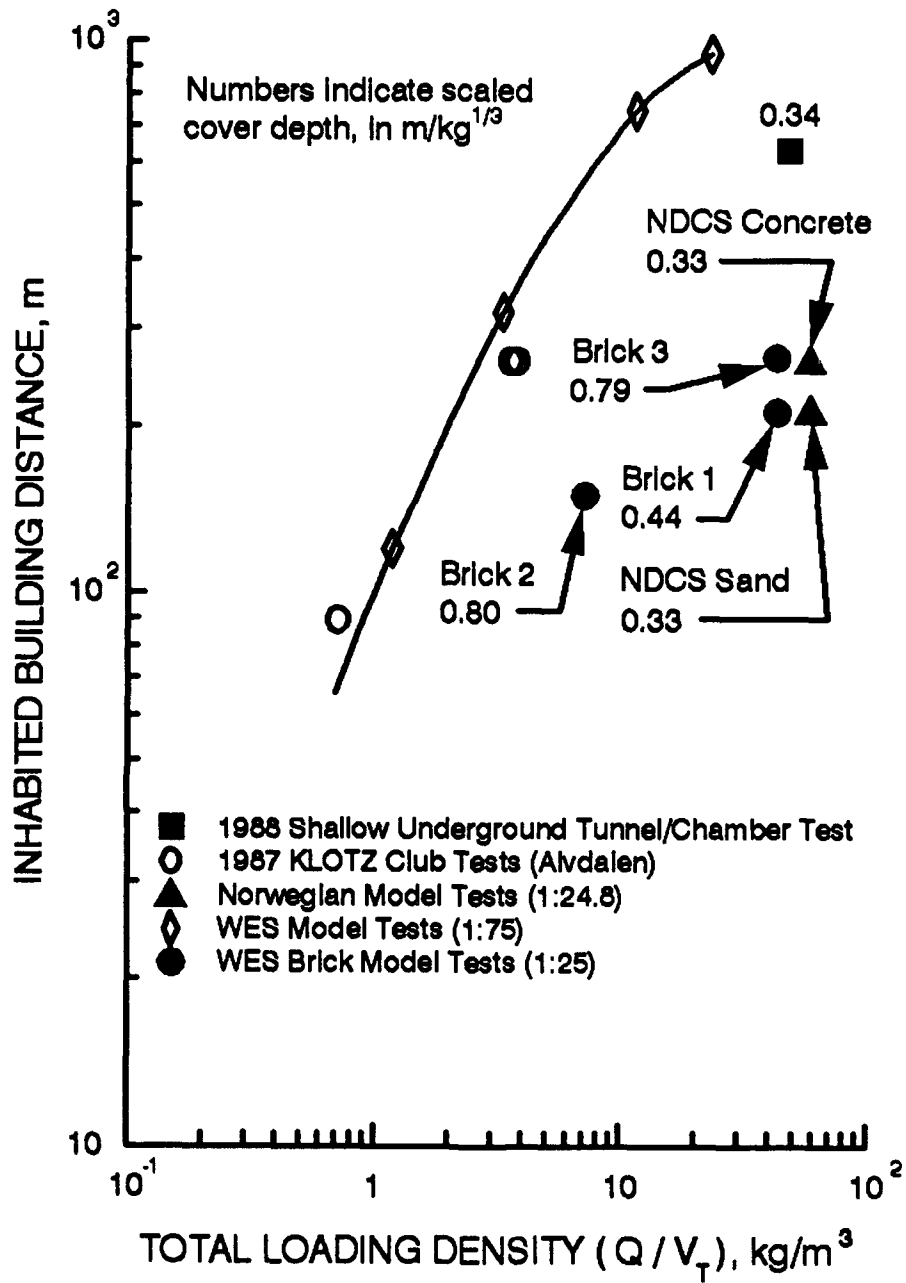


Figure 13. Airblast Inhabited Building Distance versus total loading density (charge mass divided by total internal volume) for selected model and large-scale tests. Solid symbols are for "responding" magazines, and open symbols for "non-responding" magazines.



Figure 14. Photos of debris fields from Brick Model Test 3.

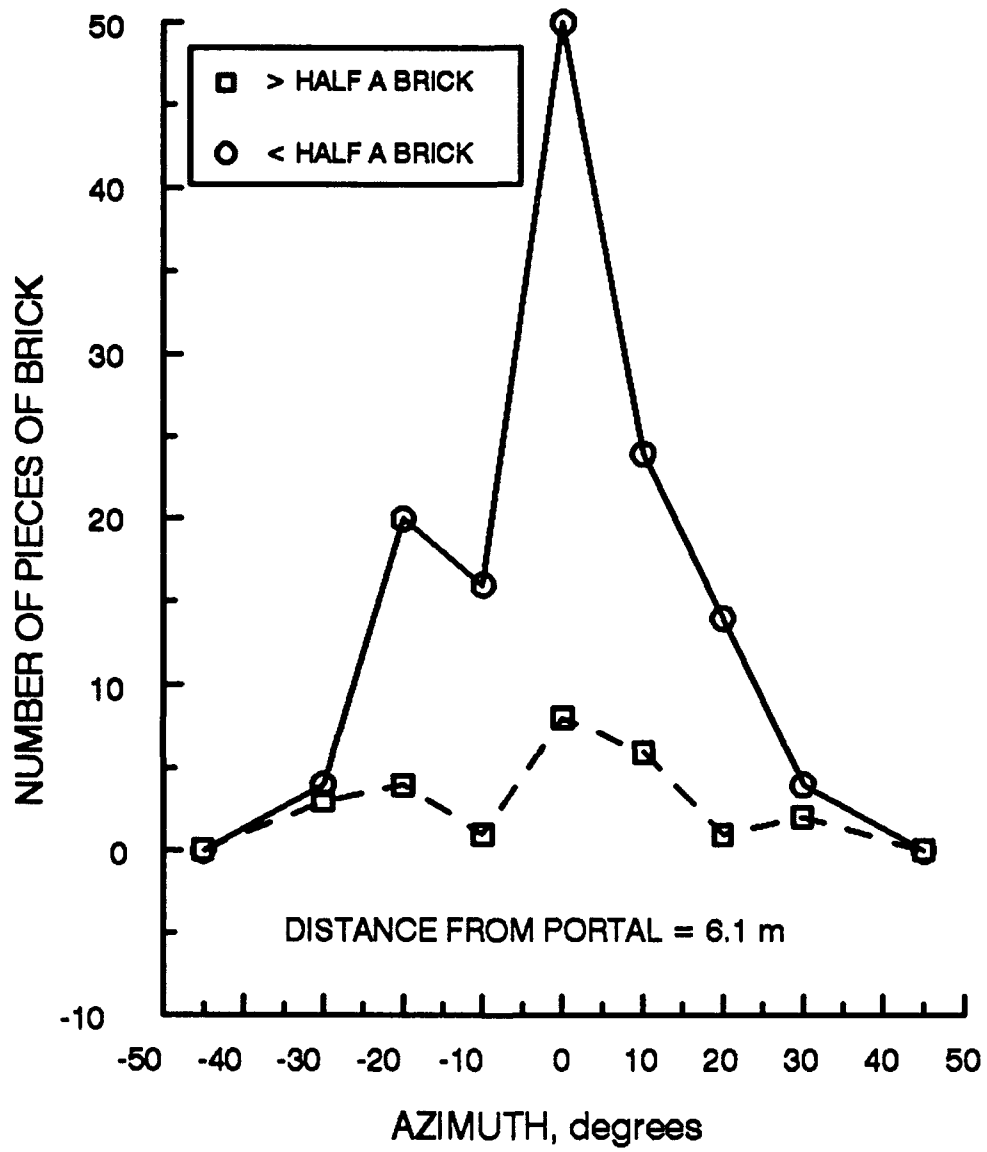


Figure 15. Ejecta distribution as a function of azimuth along the 6.1 m arc, WES Brick Model Test 3.

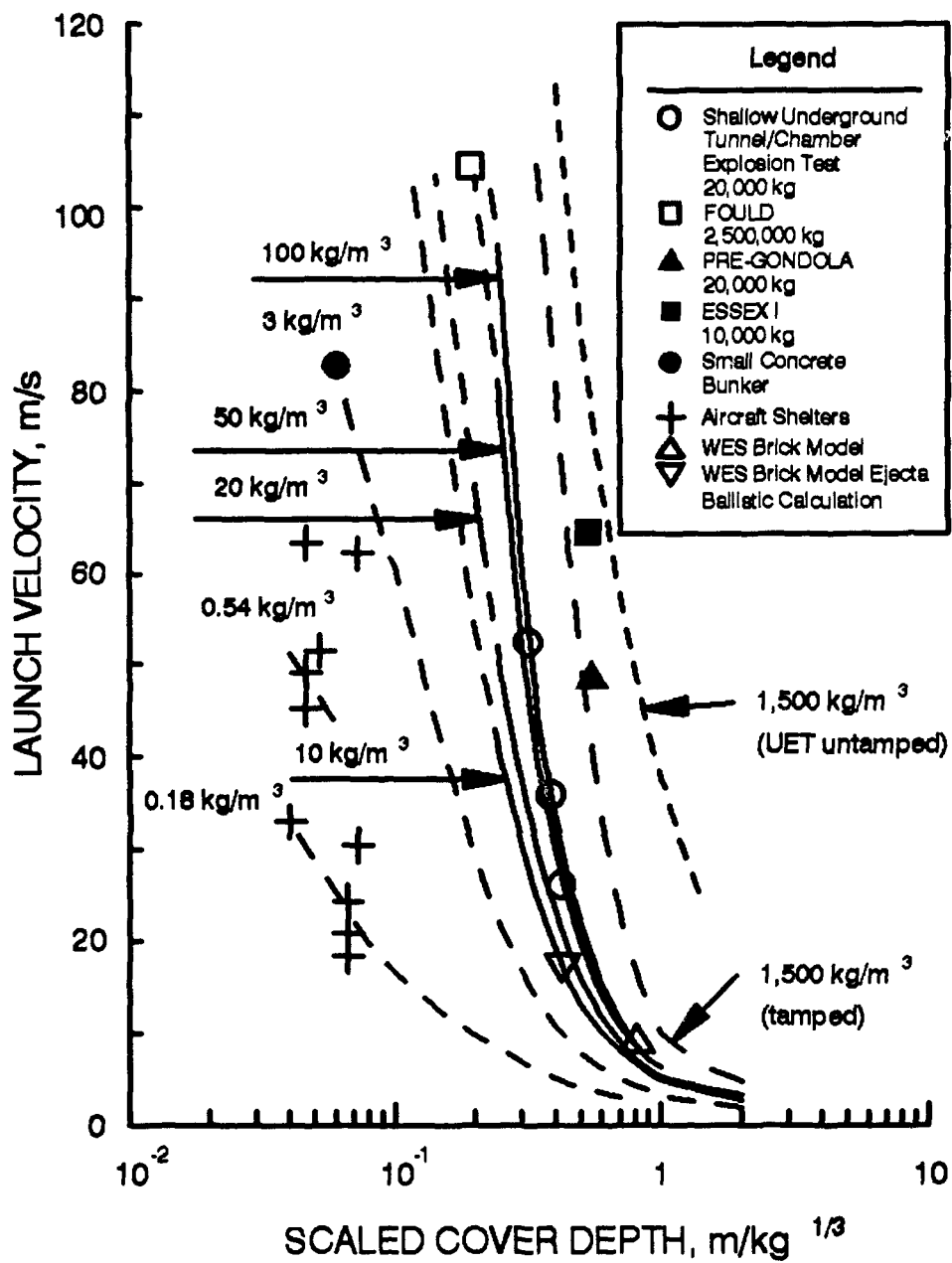


Figure 16. Launch velocity of cover rock ejecta from WES brick model test, compared to ejecta velocities from the Shallow Underground Tunnel/Chamber Explosion Test (Joachim, 1990) and other sources (Helseth, 1982) on previous explosive tests.

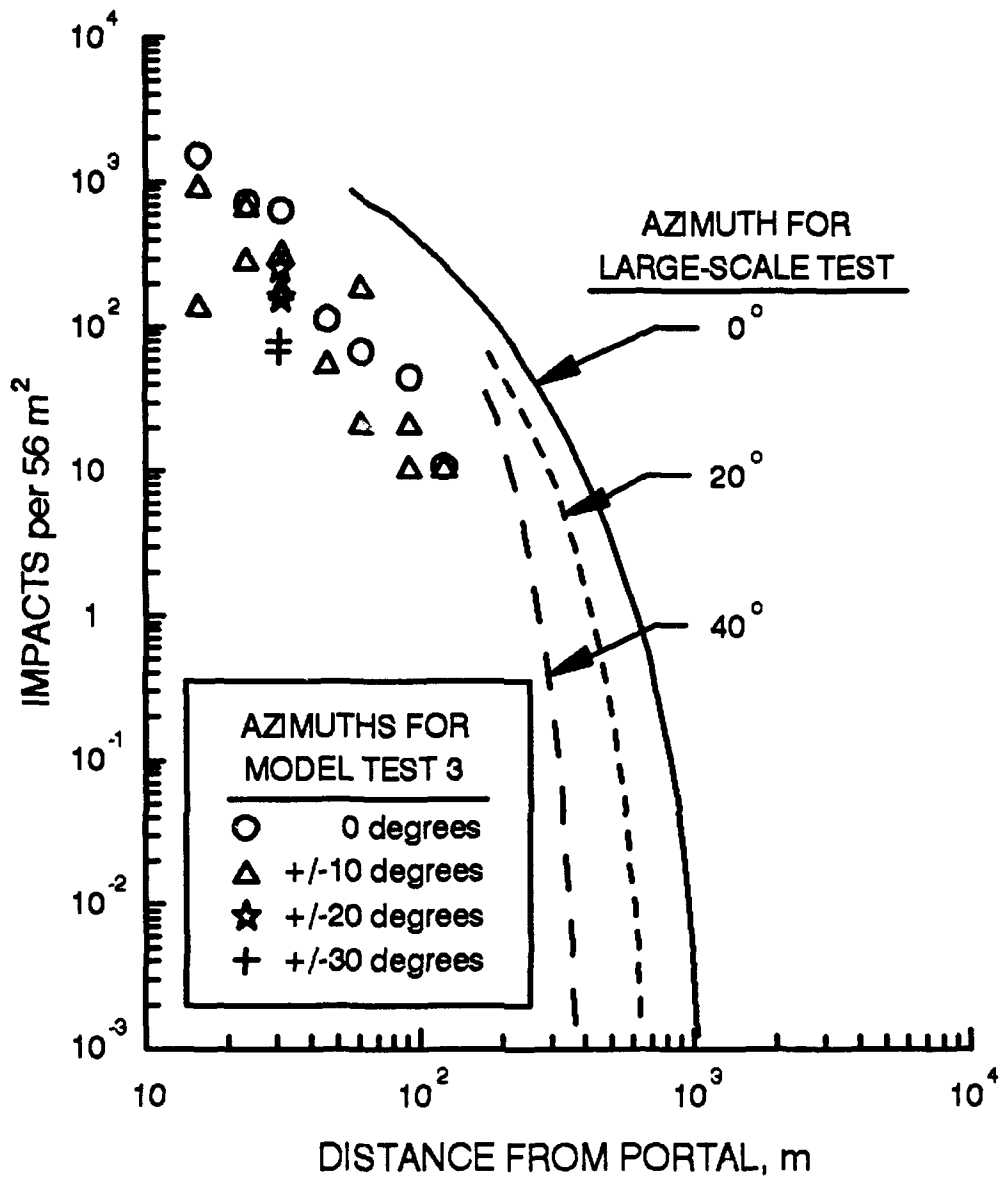


Figure 17. Relative comparison of debris densities from WES Brick Model Test 3 with the Shallow Underground Tunnel/Chamber Explosion Test (KLOTZ 1988) data curves. Distances in the model were scaled by the ratio of the charge weights taken to the one-sixth power.

Table 1. WES Brick Model Tests: Measurement Type and Gage Location Data.

Station No.	Horizontal* Distance (cm)	Elevation** (cm)	Measurement Type
AB-1	20	0	Side-on Overpressure
AB-2	20	0	Stagnation Pressure
AB-3	40	0	Side-on Overpressure
AB-4	100	0	Side-on Overpressure
AB-5	300	0	Side-on Overpressure
AB-6	600	0	Side-on Overpressure
AB-7	-10	0	Side-on Overpressure
AB-8	-50	0	Side-on Overpressure
AB-9	-124	0	Chamber Pressure
AB-10	-148	0	Chamber Pressure
GM-1	-115	52.6	Overburden Acceleration
GM-2	-125	34.3	Overburden Acceleration

* Horizontal distance along tunnel/chamber centerline measured from the tunnel portal.

** Elevation measured from the tunnel/chamber floor and/or surface of concrete airblast pad.

Table 2. WES Brick Model Tests: Explosives Charges, and Chamber Cover Thicknesses

Test No.	Explosive Charge				Minimum Scaled		
	Total Mass (kg)	Loading* Density (kg/m ³)	No. of** Strands(kg)	Length (cm)	Diameter (cm)	Chamber Cover (m/kg ^{1/3})	Portal Cover (m/kg ^{1/3})
1	1.27	60	31	48	5	0.44	0.034
2	0.21	10	5	48		0.80	0.062
3	1.27	60	31	48	5	0.79	0.49

* Mass of explosives divided by chamber volume.

** 0.085 kg/m (400 grains/foot) detonation cord

Table 3. WES Brick Model Tests: Airblast Pressure and Ground Shock Measurements; Test 1 (60 kg/m³ PETN charge loading density, 0.44 m/kg^{1/3} scaled chamber cover depth).

Station No.	Horizontal* Distance (cm)	Elevation** (cm)	Arrival Time (msec)	Peak Data	
				Measured	First Integral
AB-1	20	0	0.77	5.37 MPa	2.0 kPa-sec
AB-2 [!]	20	2.5	0.67	1.83 MPa	1.1 kPa-sec
AB-3	40	0	0.83	1.92 MPa	0.10 kPa-sec
AB-4	100	0	----	----	----
AB-5	300	0	5.6	0.036 MPa	28. Pa-sec
AB-6	600	0	13.5	0.010 MPa	13. Pa-sec
AB-7	-10	0	----	----	----
AB-8	-50	0	0.17	12.4 MPa	----
AB-9	-124	8	----	----	----
AB-10	-148	8	0.2	>750 MPa	----
GM-1	-115	52.6	0.24	----	----
GM-2	-125	34.3	----	----	----

* Horizontal distance along tunnel/chamber centerline measured from the tunnel portal. Negative distances are inside tunnel or above chamber cover.

** Elevations measured from the tunnel/chamber floor.

! Total pressure measurement

Table 4. WES Brick Model Tests: Airblast Pressure and Ground Shock Measurements; Test 2 (10 kg/m³ PETN charge loading density, 0.80 m/kg^{1/3} scaled chamber cover depth).

Station No.	Horizontal* Distance (cm)	Elevation** (cm)	Arrival Time (msec)	Peak Data	
				Measured	First Integral
AB-1	20	0	0.88	>5.2 MPa	>0.57 kPa-sec
AB-2 [!]	20	2.5	1.35	1.13 MPa	1.1 kPa-sec
AB-3	40	0	1.09	0.45 MPa	78. Pa-sec
AB-4	100	0	2.33	0.125 MPa	64. Pa-sec
AB-5	300	0	7.04	16. kPa	19. Pa-sec
AB-6	600	0	15.3	5.2 kPa	6.0 Pa-sec
AB-7	-10	0	0.64	1.89 MPa	1.9 kPa-sec
AB-8	-50	0	0.37	2.0 Mpa	1.0 kPa-sec
AB-9	-124	8	----	114. MPa	3.4 kPa-sec
AB-10	-148	8	----	52. MPa	4.0 kPa-sec
GM-1	-115	52.6	0.25	1500 g's	1.08 m/sec
GM-2	-125	34.3	0.06	1500 g's	2.0 m/sec

* Horizontal distance along tunnel/chamber centerline measured from the tunnel portal.

** Elevations measured from the tunnel/chamber floor.

! Total pressure measurement

Table 5. WES Brick Model Tests: Airblast Pressure and Ground Shock Measurements; Test 3 (60 kg/m³ PETN charge loading density, 0.79 m/kg^{1/3} scaled chamber cover depth).

Station No.	Horizontal* Distance (cm)	Elevation** (cm)	Arrival Time (msec)	Peak Data	
				Measured	First Integral
AB-1	20	0	0.45	4.8 MPa	0.75 kPa-sec
AB-2 [!]	20	2.5	0.77	2.8 MPa	----
AB-3	40	0	0.60	2.2 MPa	0.16 kPa-sec
AB-4	100	0	1.30	0.78 MPa	0.10 kPa-sec
AB-5	300	0	5.0	0.049 MPa	63. Pa-sec
AB-6	600	0	12.7	0.015 MPa	20. Pa-sec
AB-7	-10	0	0.33	6.3 MPa	----
AB-8	-50	0	0.16	29. MPa	----
AB-9	-124	8	----	----	----
AB-10	-148	8	----	----	----
GM-1	-115	52.6	0.16	----	----
GM-2	-125	34.3	----	----	----

* Horizontal distance along tunnel/chamber centerline measured from the tunnel portal.

** Elevations measured from the tunnel/chamber floor.

! Total pressure measurement

Table 6. Effects of Magazine Cover Resistance on Airblast

Model Test	Model Scale	Cover Type	Scaled Cover Depth m/kg ^{1/2}	Loading Density m/kg ³	Airblast Effects	
					Portal Pressure MPa	Full-Scale IBD m
NDCS Sand	1:24.8	Sand	0.33	58.3	6.2	208
Brick Model 1	1:25	Bricks	0.44	60.	5.0	205
NDCS Concrete	1:24.8	Concrete	0.33	58.3	103.	250
Brick Model 3	1:25	Bricks	0.79	60.	5.0	250
WES Concrete	1:75	Concrete	>2.0	60.	---	1000

Extrapolated from Figure 13.

Table 7. WES Brick Model Test 3: Brick Ejecta
Distributions.

Horizontal* Distance (m)	Azimuth** (degrees)	Number of Brick Ejecta Size of Brick	
		Full>Half	<Half
3.1	0	4	134
4.6	0	3	62
6.1	0	8	50
9.1	0	1	9
12.2	0	2	4
18.3	0	0	4
24.4	0	0	1
3.1	10	0	13
4.6	10	3	24
6.1	10	6	24
9.1	10	0	5
12.2	10	1	16
18.3	10	0	2
24.4	10	1	0
3.1	350	2	84
4.6	350	3	60
6.1	350	1	16
9.1	350	3	2
12.2	350	0	2
18.3	350	0	1
24.4	350	0	0
6.1	20	1	14
6.1	30	2	4
6.1	45	0	0
6.1	340	4	20
6.1	330	3	4
6.1	315	0	0

* Horizontal distance along tunnel/chamber
Centerline measured from the tunnel portal.

** Azimuth referenced to extended tunnel/chamber
centerline.

APPENDICES A, B AND C

AIRBLAST PRESSURE AND GROUND MOTION WAVE FORMS

Gage Identification Code:

Digital Gage	MUST	00-X	CBS	0	0000	0.0000
Array Size	MN					
F1 Low Pass	0000	HZ				
Cal Val	00.0					
Deflection	0000					
		00	KHZ			
				DD-MM-YY		

The first line contains identification code (00-X). AB and GM identify airblast and ground motion (acceleration) measurements, respectively. In addition, some time histories require baseline shifting indicated by the CBS (constant baseline shift) shown on the far right of the first line. The numbers following the CBS indicate shift starting and ending times (msec) and the amount that the data was shifted. Negative numbers indicate a downward shifting of the time history. The second line gives the size of the data sample. The third line lists the low pass filter cutoff frequency. The fourth and fifth lines gives the values of the shunt calibration and the corresponding value of the voltage deflection, respectively. The last line shows the sampling frequency of the filtered data and the date on which the plot was generated.

APPENDIX A

AIRBLAST AND GROUND MOTION WAVE FORMS

Brick Model Test 1

Explosives Charge: 1.27 kg PETN

Chamber Loading Density: 60 kg/m³

Minimum Scaled Chamber Cover Depth: 0.44 m/kg^{1/3}

Digital Gage MUST AB-1 CBS 0 20 -0.00280
 Array Size: 200050
 Stop at 1.5
 Cal val 570.7
 Deflection -1536
 Model Underground Storage Test
 Test 1
 1000 KHZ 28-FEB-91

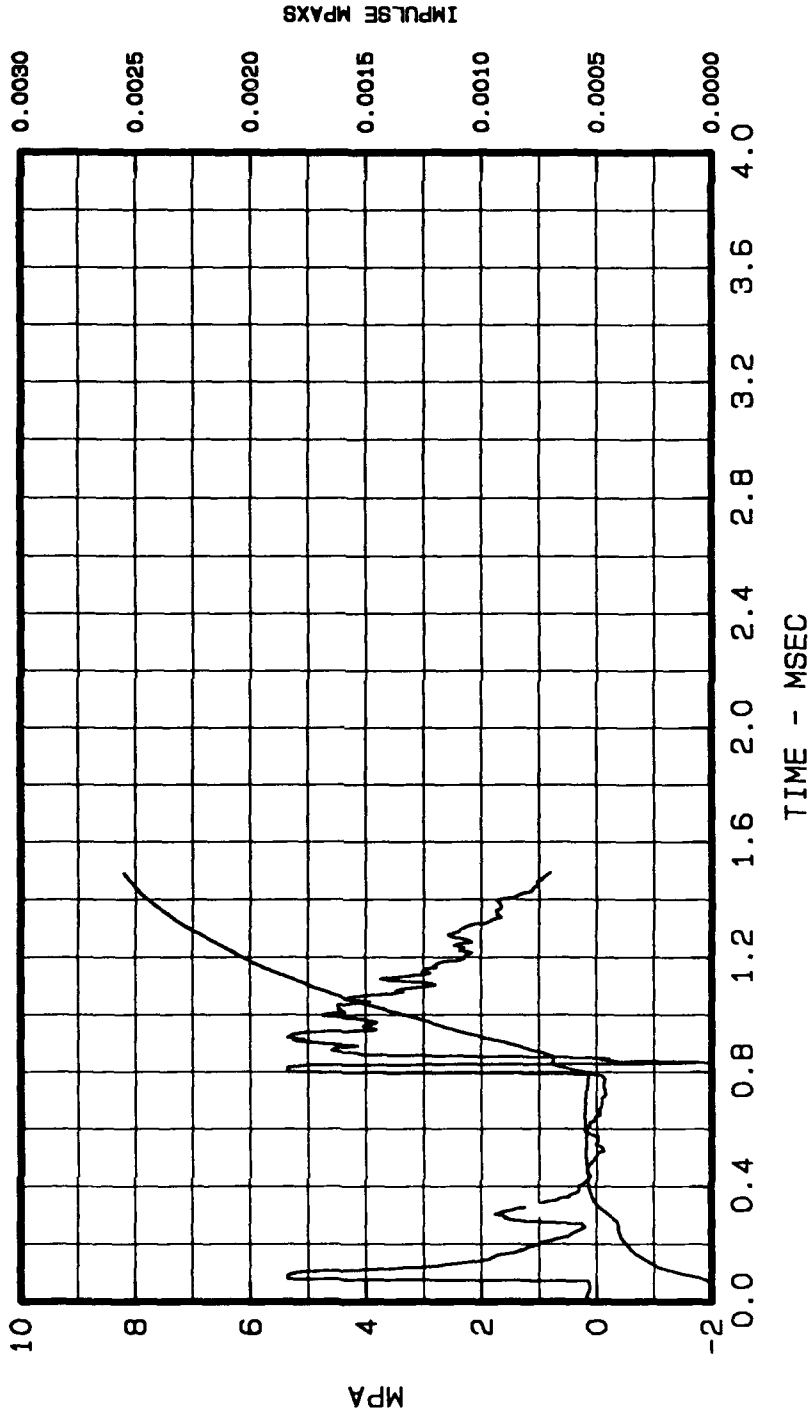


Figure A.1 WES Brick Model Test 1: Gage AB-1, free-field overpressure-time history at 20 cm from tunnel portal.

Digital Gage
Array Size: 200050
Stop at 2.130
Cal val 3551
Deflection -1538

MUST AB-2

Model Underground Storage Test
Test 1

1000 KHZ 28-FEB-91

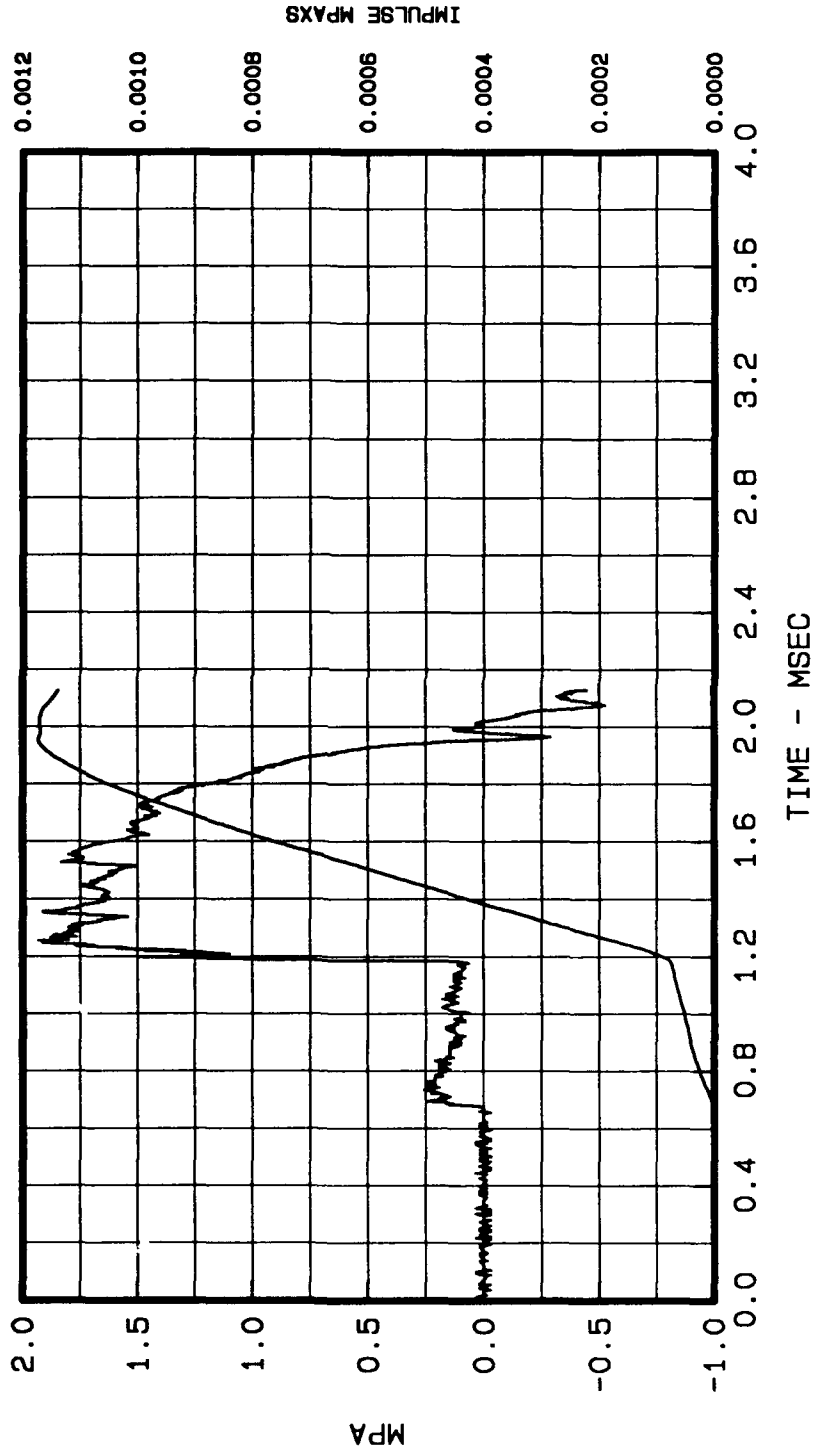


Figure A.2 WES Brick Model Test 1: Gage Ab-2, stagnation pressure-time history at 20 cm from tunnel portal.

Digital Gage
 Array Size: 200050
 Stop at 3.9
 Cal val 260.1
 Deflection -1595

MUST AB-3
 Model Underground Storage Test
 Test 1
 1000 KHZ 28-FEB-91

C98 0 20 -0.000183

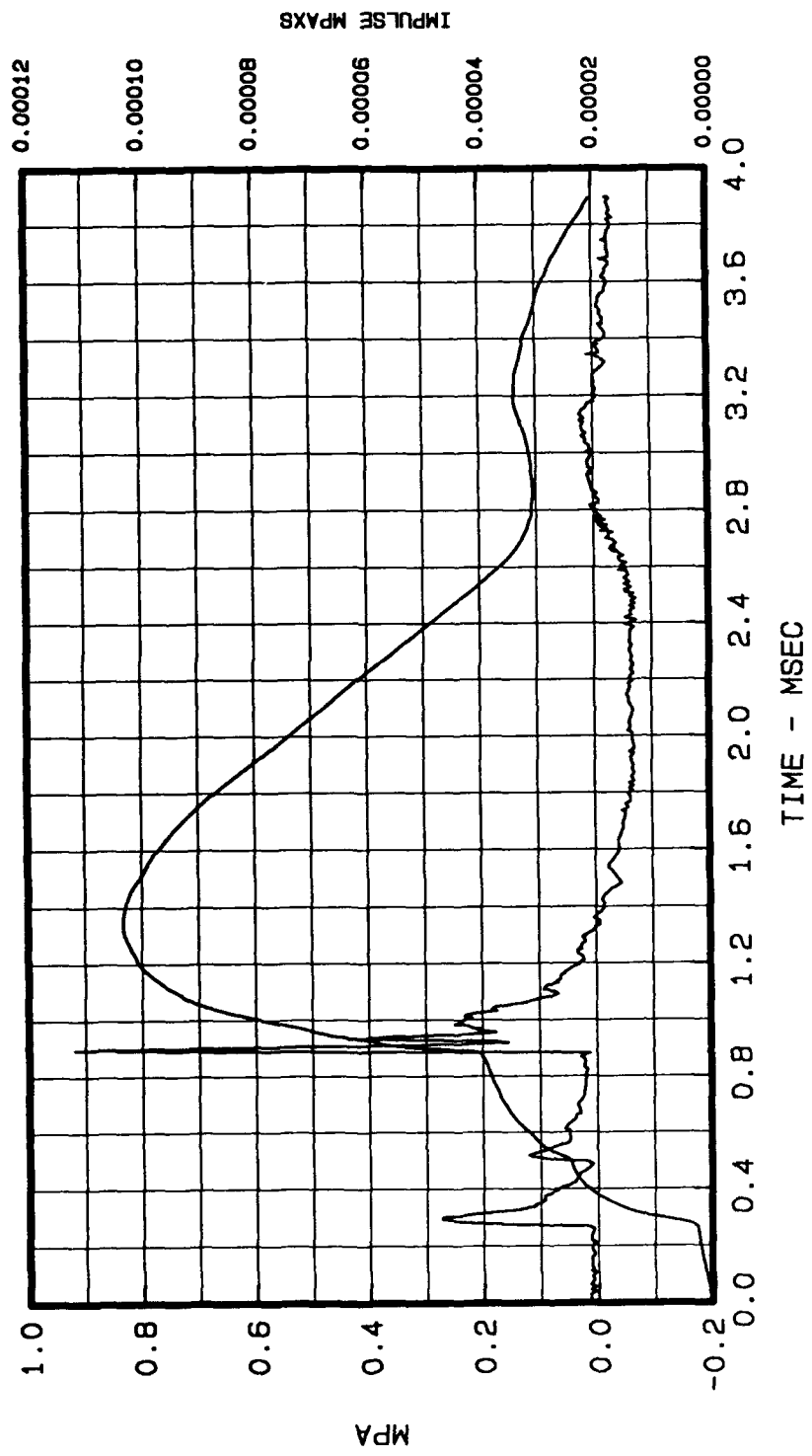


Figure A.3 WES Brick Model Test 1: Gage AB-3, free-field overpressure-time history at 40 cm from tunnel portal.

Digital Gage
 Array Size: 200050
 Cal val 13.4
 Deflection -1535

MUST AB-5
 Model Underground Storage Test
 Test 1
 1000 KHZ 8-DEC-89

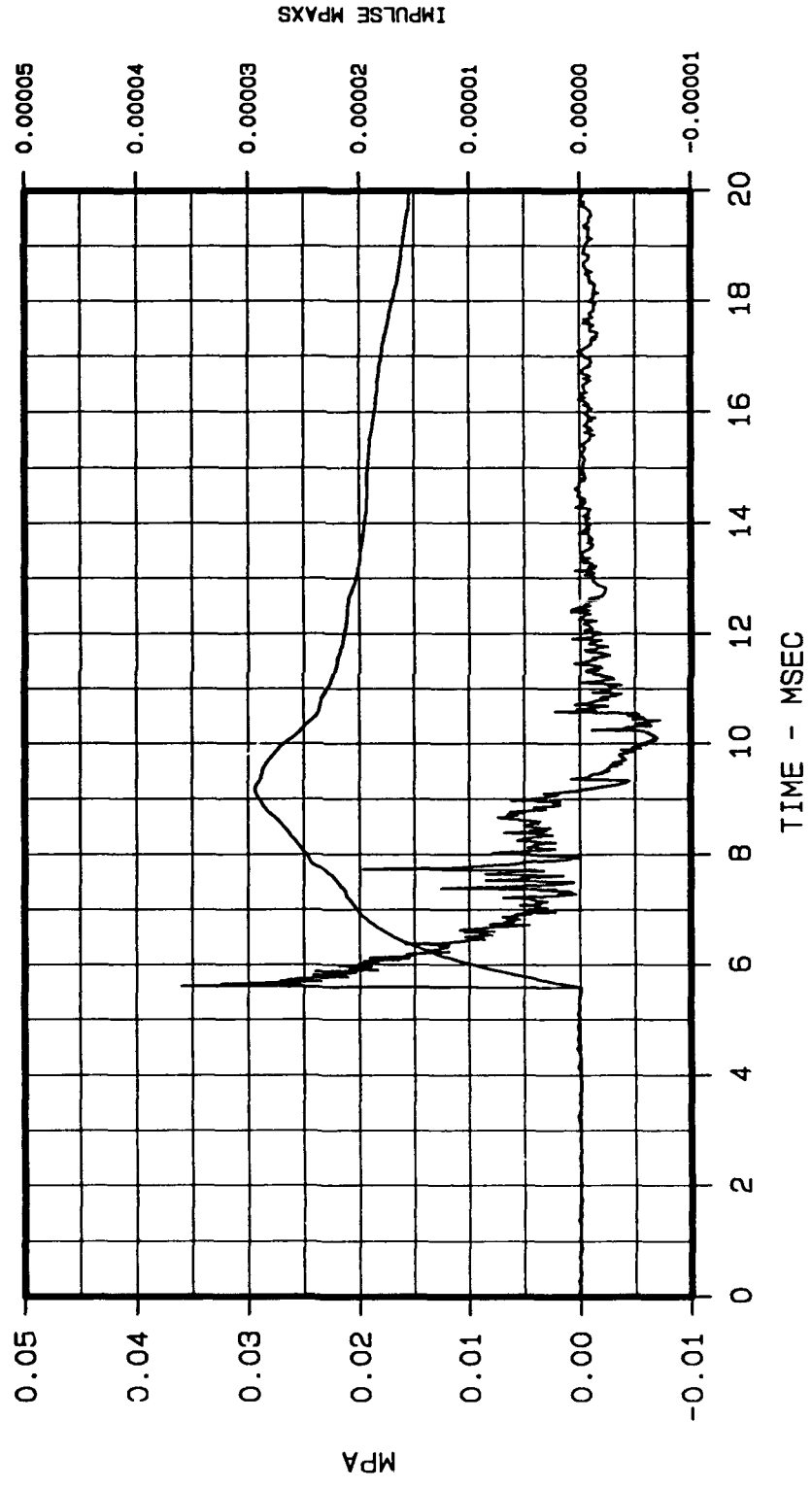


Figure A.4 WES Brick Model Test 1: Gage AB-5, free-field overpressure-time history at 3 m from tunnel portal.

Digital Gage
Array Size: 200050
Cal val 4.4
Deflection -1583

MUST AB-6

Model Underground Storage Test

Test 1

1000 KHZ 30-OCT-90

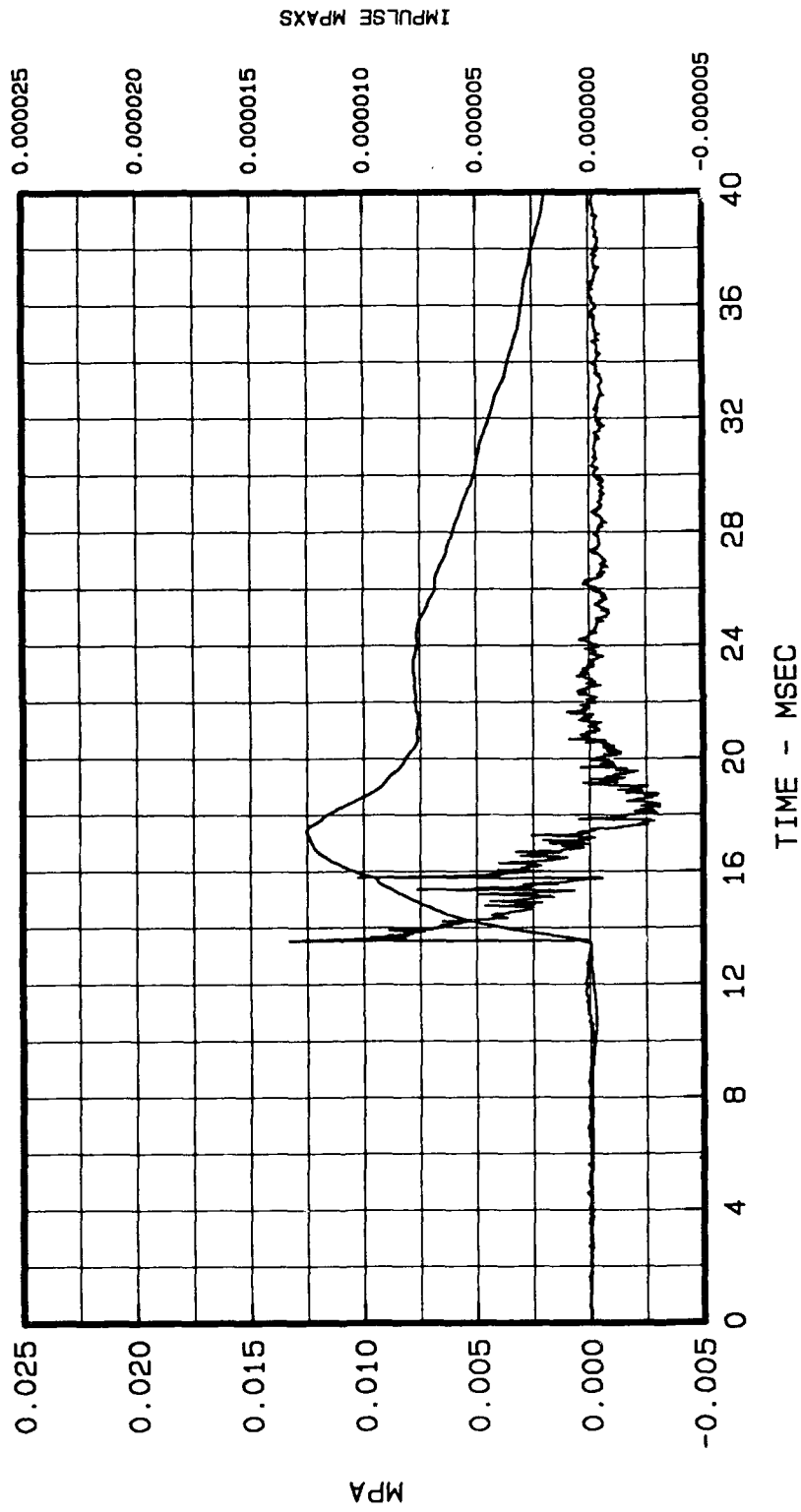


Figure A.5 WES Brick Model Test 1: Gage AB-6, free-field overpressure-time history at 6 m from tunnel portal.

Digital Gage
 Array Size: 200050
 Stop at 1.4
 Cal vel 1612.9
 Deflection -1525

MUST AB-8
 Model Underground Storage Test
 Test 1
 1000 KHZ 28-FEB-91

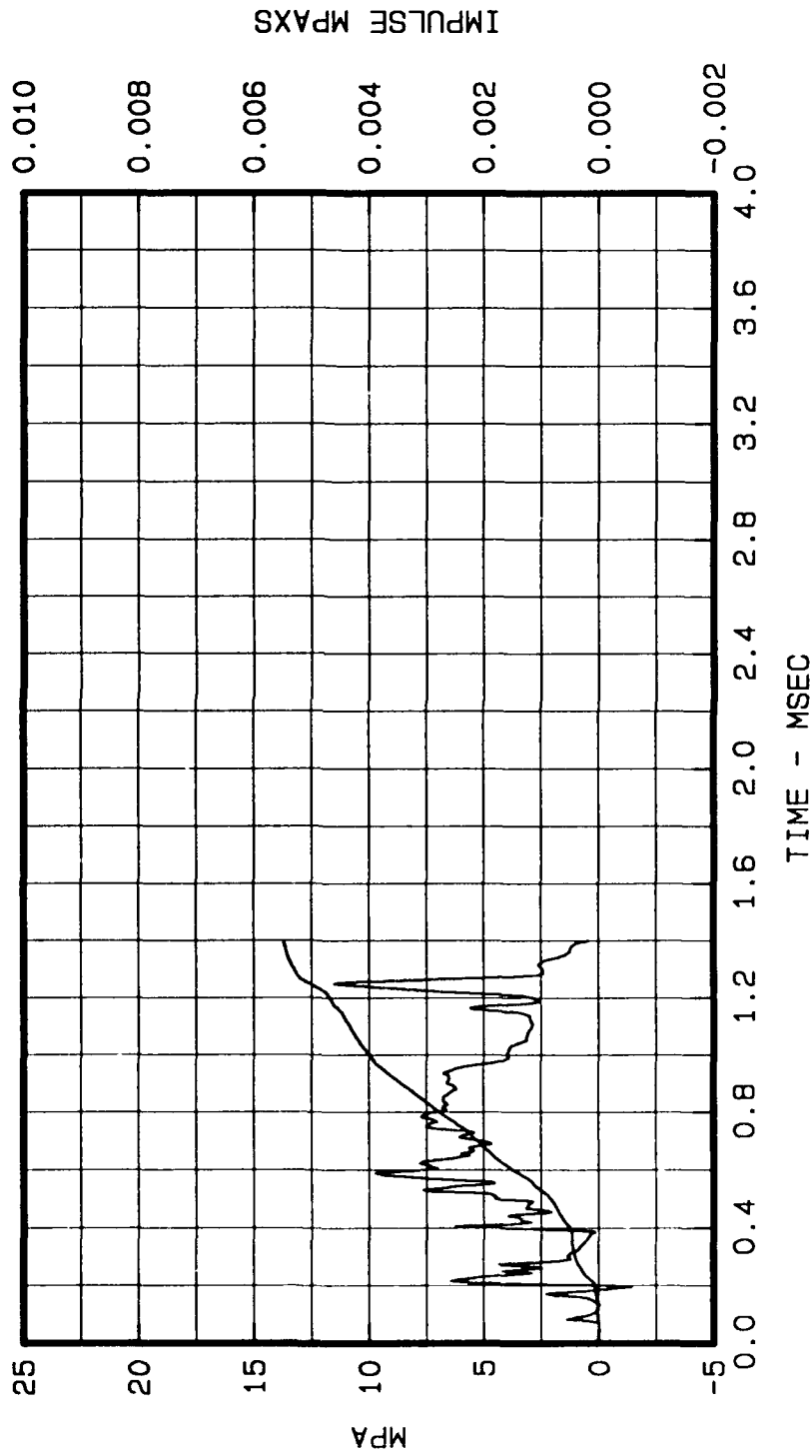


Figure .6 WES Brick Model Test 1: Gage AB-8, access tunnel overpressure-time history at 50 cm from tunnel portal.

Digital Gage
Array Size: 200050
Cal val 4405
Deflection -1525

MUST CM-1

Model Underground Storage Test

Test 1

1000 KHZ 5-NOV-90

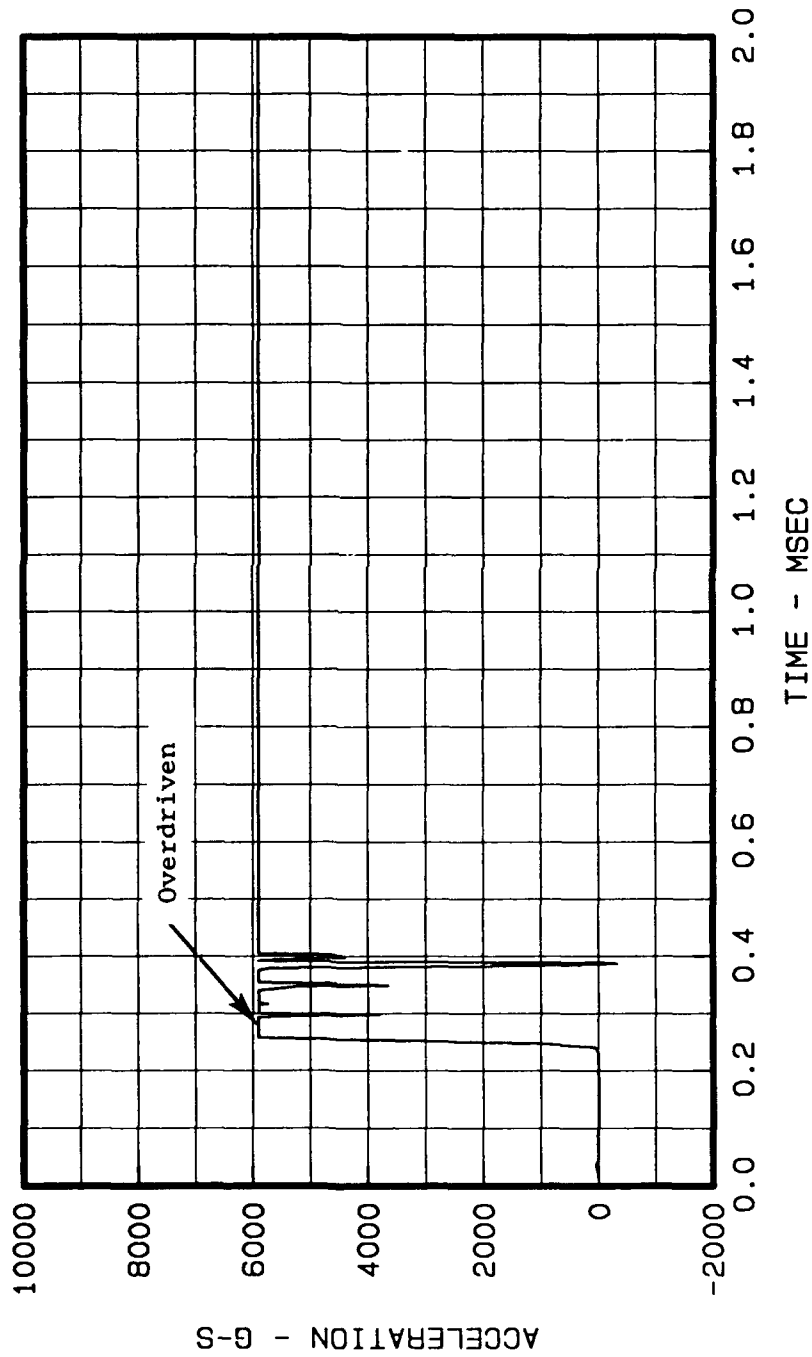


Figure A.8 WES Brick Model Test 1: Gage CM-1, overgurdan acceleration-time history at 18.3 cm above chamber roof.

APPENDIX B

AIRBLAST AND GROUND MOTION WAVE FORMS

Brick Model Test 2

Explosives Charge: 0.21 kg PETN

Chamber Loading Density: 10 kg/m³

Minimum Scaled Chamber Cover Depth: 0.80 m/kg^{1/3}

Digital Gage
Array Size: 200050
Cal val 570.7
Deflection -1555

MUST AB-1

Model Underground Storage Test

Test 2

1000 KHZ 21-NOV-89

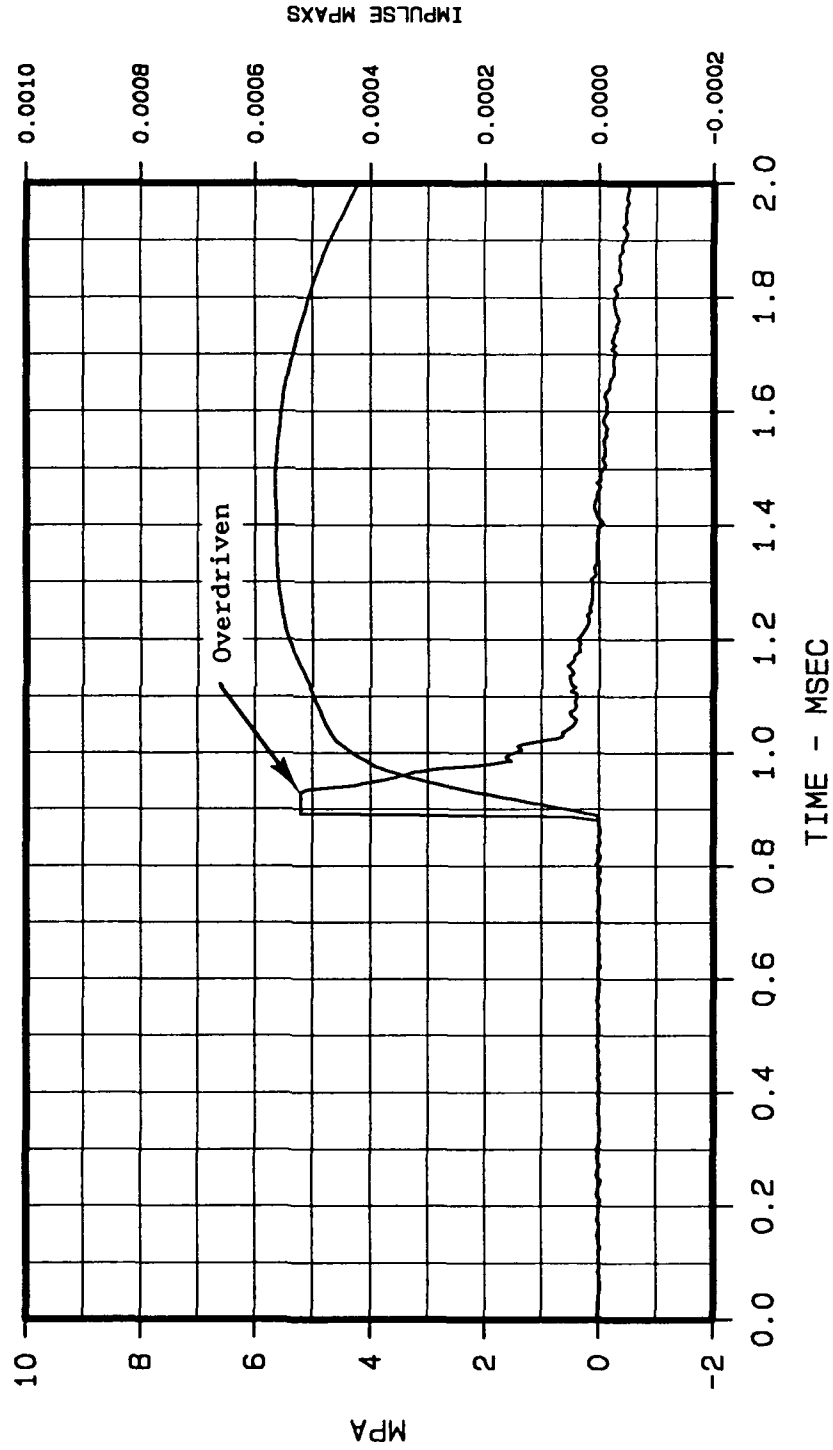


Figure B.1 WES Brick Model Test 2: Gage AB-1, free-field overpressure-time history at 20 cm from tunnel portal.

Digital Gage
Array Size: 200050
Cal val 1091.5
Deflection -1524

MUST AB-2

Model Underground Storage Test

Test 2

1000 KHZ 21-NOV-89

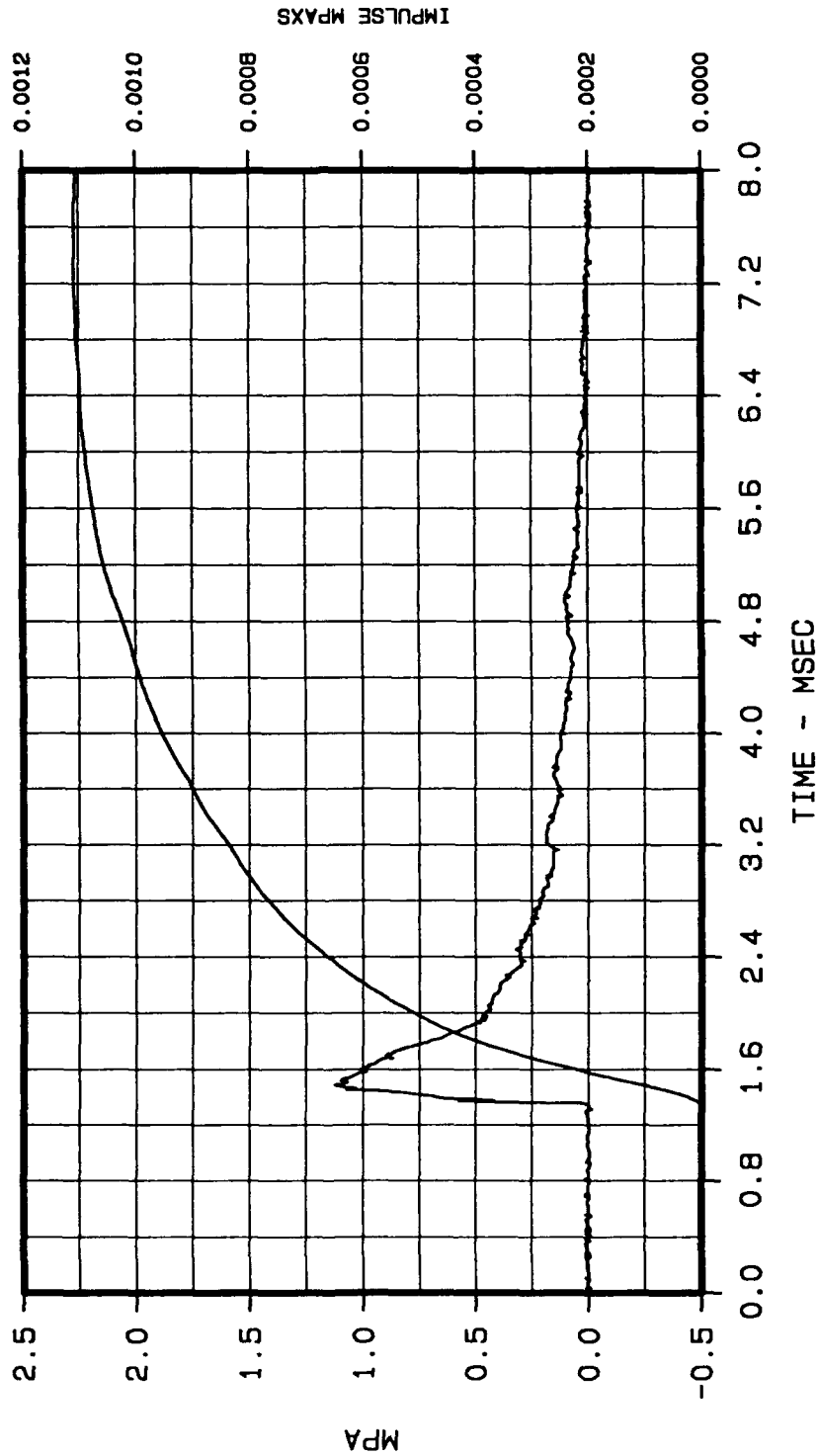


Figure B.2 WES Brick Model Test 2: Gage AB-2, stagnation pressure-time history at 20 cm from tunnel portal.

Digital Gage
Array Size: 200050
Cal Val 260.1
Deflection -1509

MUST AB-3

Model Underground Storage Test

Test 2

1000 KHZ 21-NOV-89

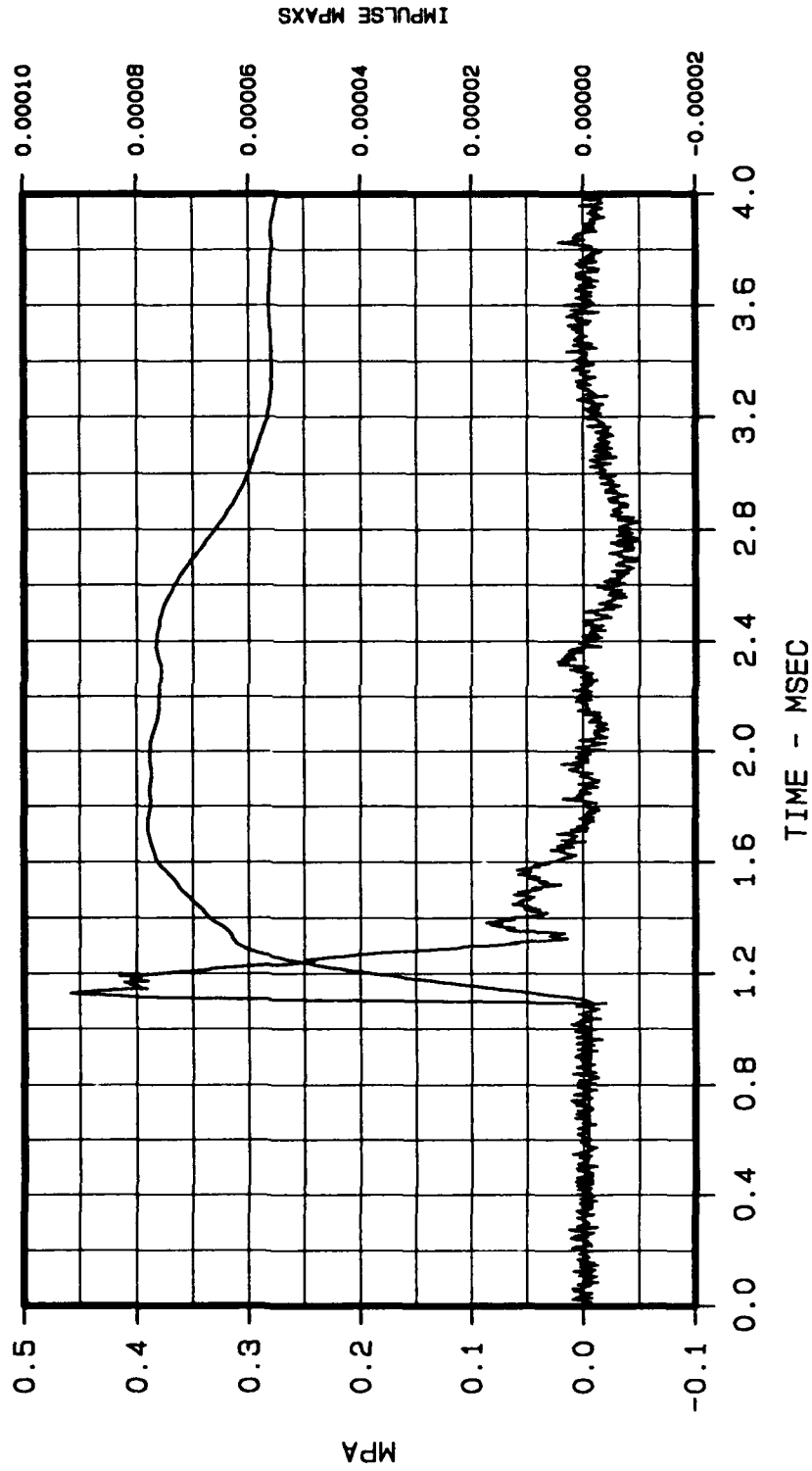


Figure B.3 WES Brick Model Test 2: Gage AB-3, free-field overpressure-time history at 40 cm from tunnel portal.

Digital Gage
Array Size: 200050
Cal val 238.8
Deflection -1521

MUST AB-4

Model Underground Storage Test

Test 2

1000 KHZ 30-OCT-90

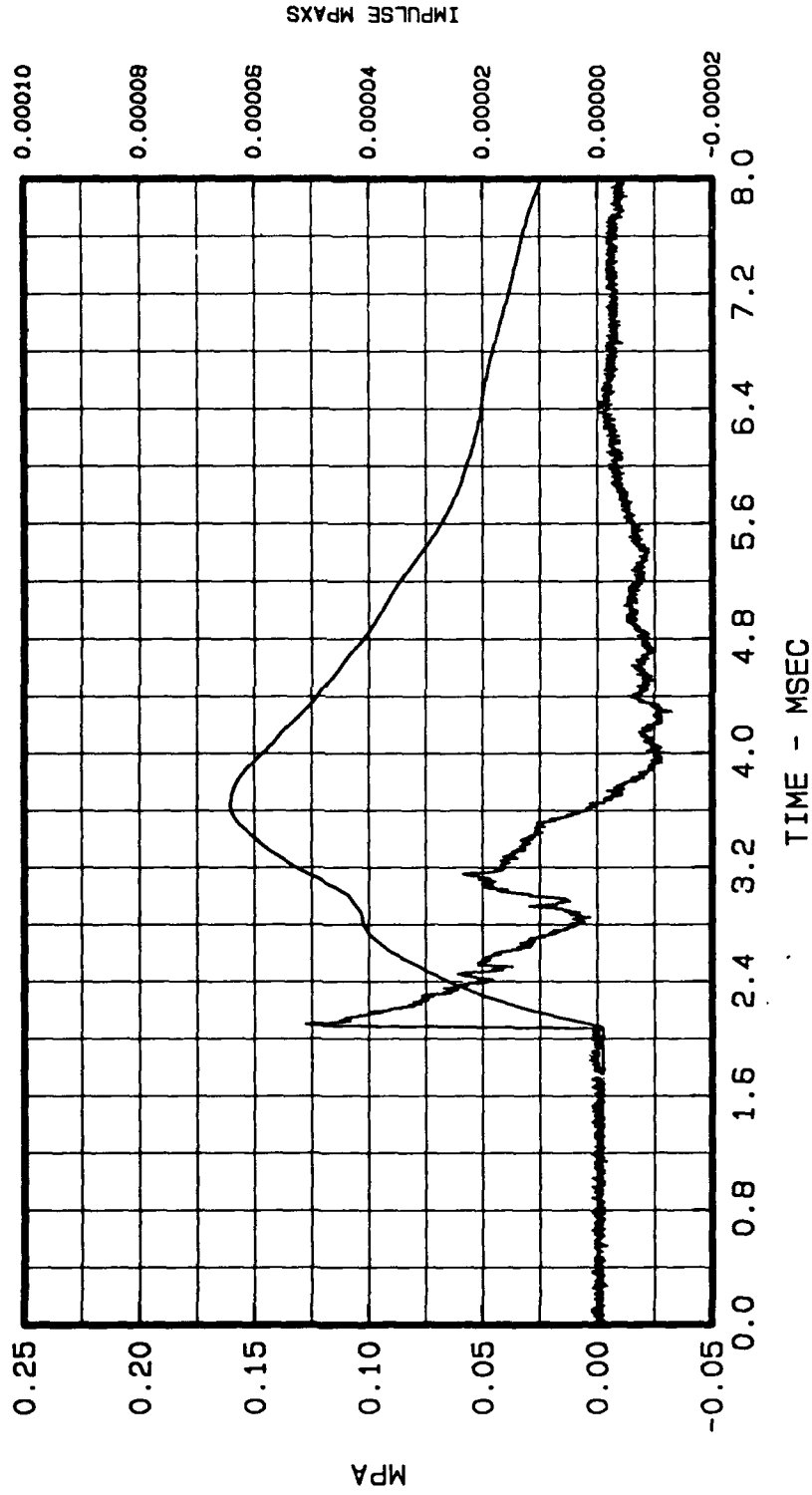


Figure B.4 WES Brick Model Test 2: Gage AB-4, free-field overpressure-time history at 1 m from tunnel portal.

Digital Gage
Array Size: 200050
Cal vel 13.4
Deflection -1536

MUST AB-5

Model Underground Storage Test

Test 2

1000 KHZ 30-OCT-90

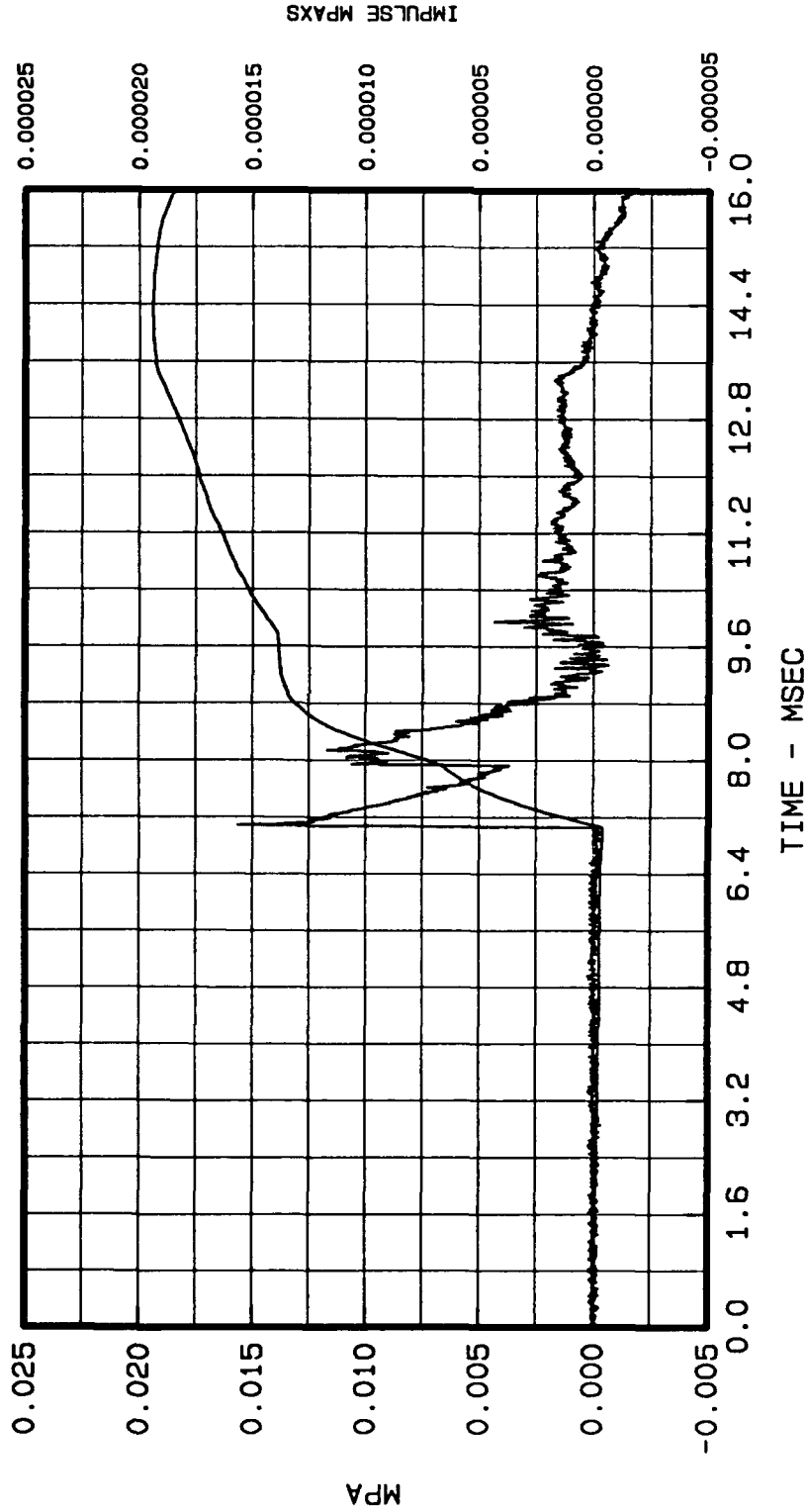


Figure B.5 WES Brick Model Test 2: Gage AB-5, free-field overpressure-time history at 3 m from tunnel portal.

Digital Gage
Array Size: 20050
Cal val 6.4
Deflection -1524

MJST AB-6

Model Underground Storage Test

Test 2

1000 KHZ 30-OCT-90

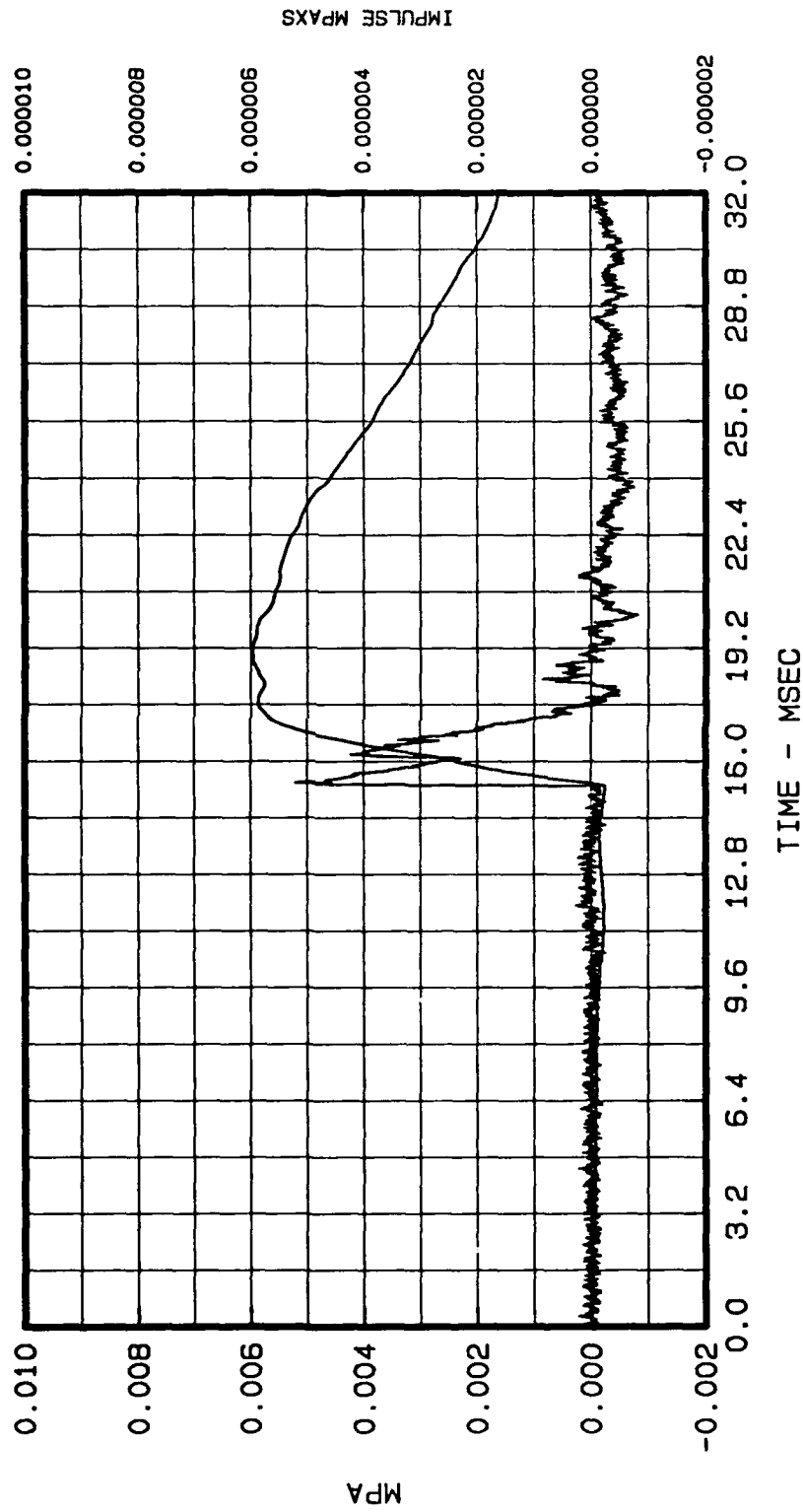


Figure B.6 WES Brick Model Test 2: Gage AB-6, free-field overpressure-time history at 6 m from tunnel portal.

Digital Gage
Array Size: 200050
Cal vel 4422
Deflection -1530

MUST AB-7

Model Underground Storage Test

Test 2

1000 KHZ 30-OCT-90

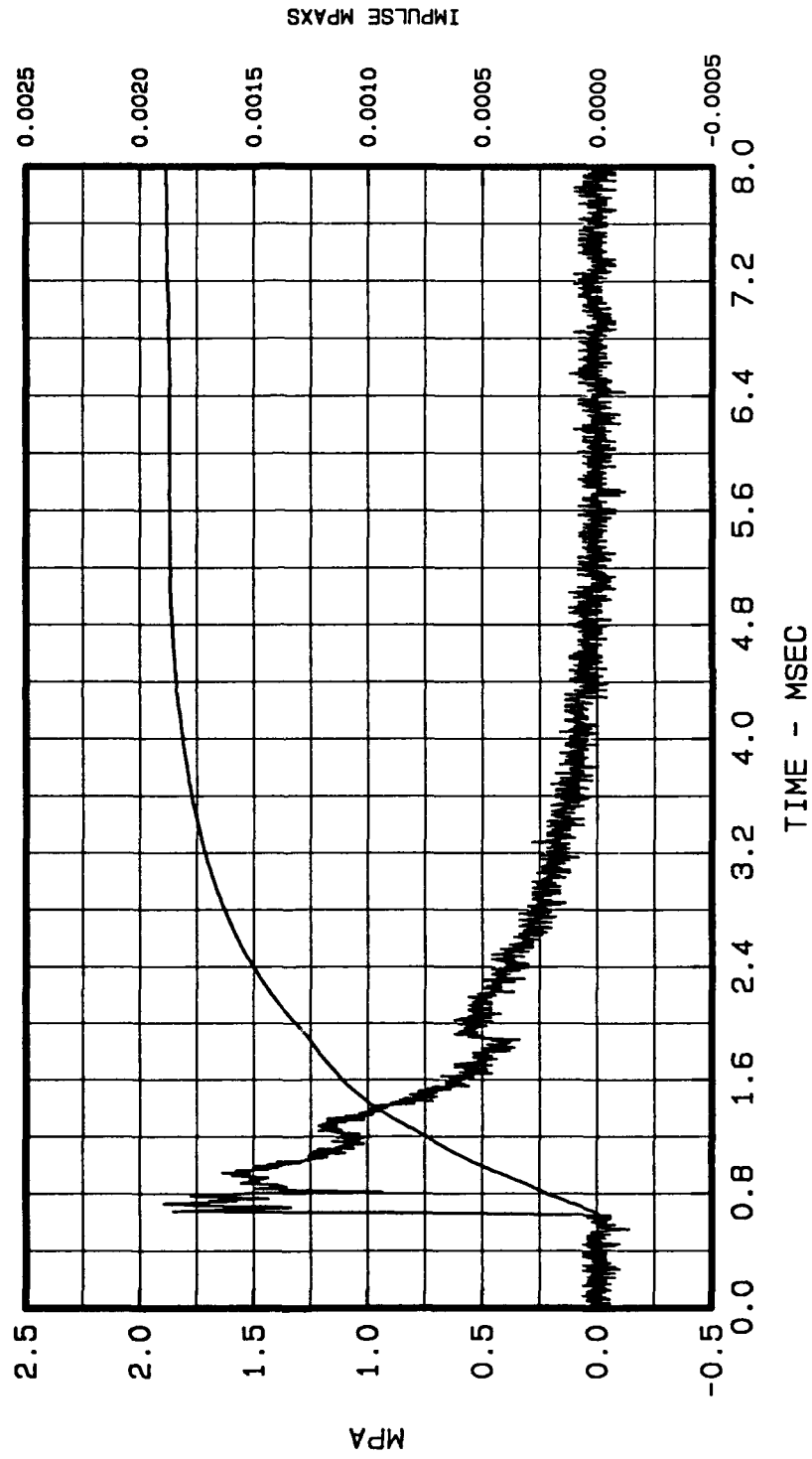


Figure B.7 WES Brick Model Test 2: Gage AB-7, access tunnel overpressure-time history at 10 cm from portal.

Digital Gage
Array Size: 200050
Cal val 4870
Deflection -1528

MUST AB-8

Model Underground Storage Test

Test 2

1000 KHZ 30-OCT-90

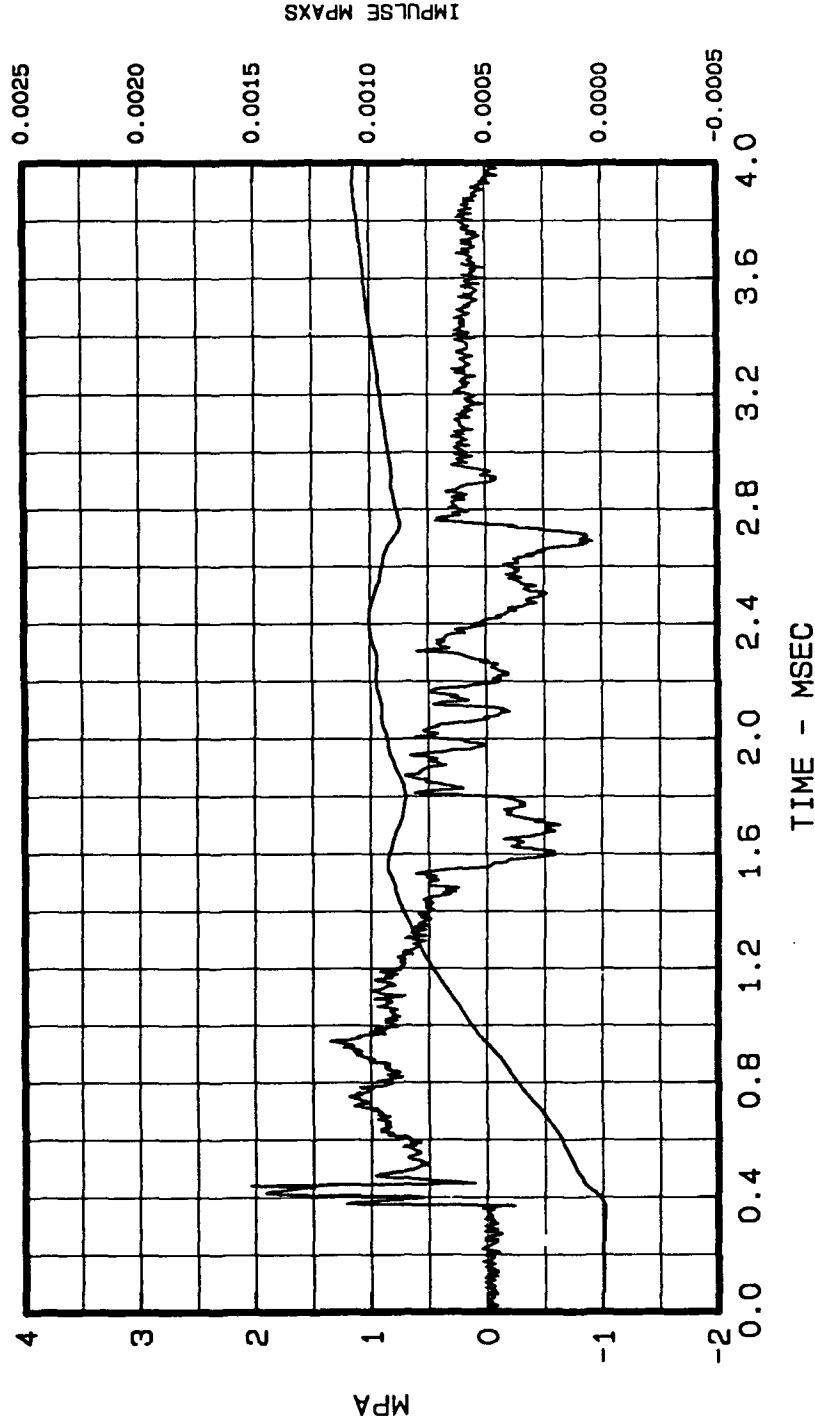


Figure B.8 WES Brick Model Test 2: Gage AB-8, access tunnel overpressure-time history at 50 cm from portal.

Digital Gage
Array Size: 200050
Stop at 0.25
Cal val 80000
Deflection 1548

MUST AB-9

Model Underground Storage Test

Test 2

1000 KHZ 5-NOV-90

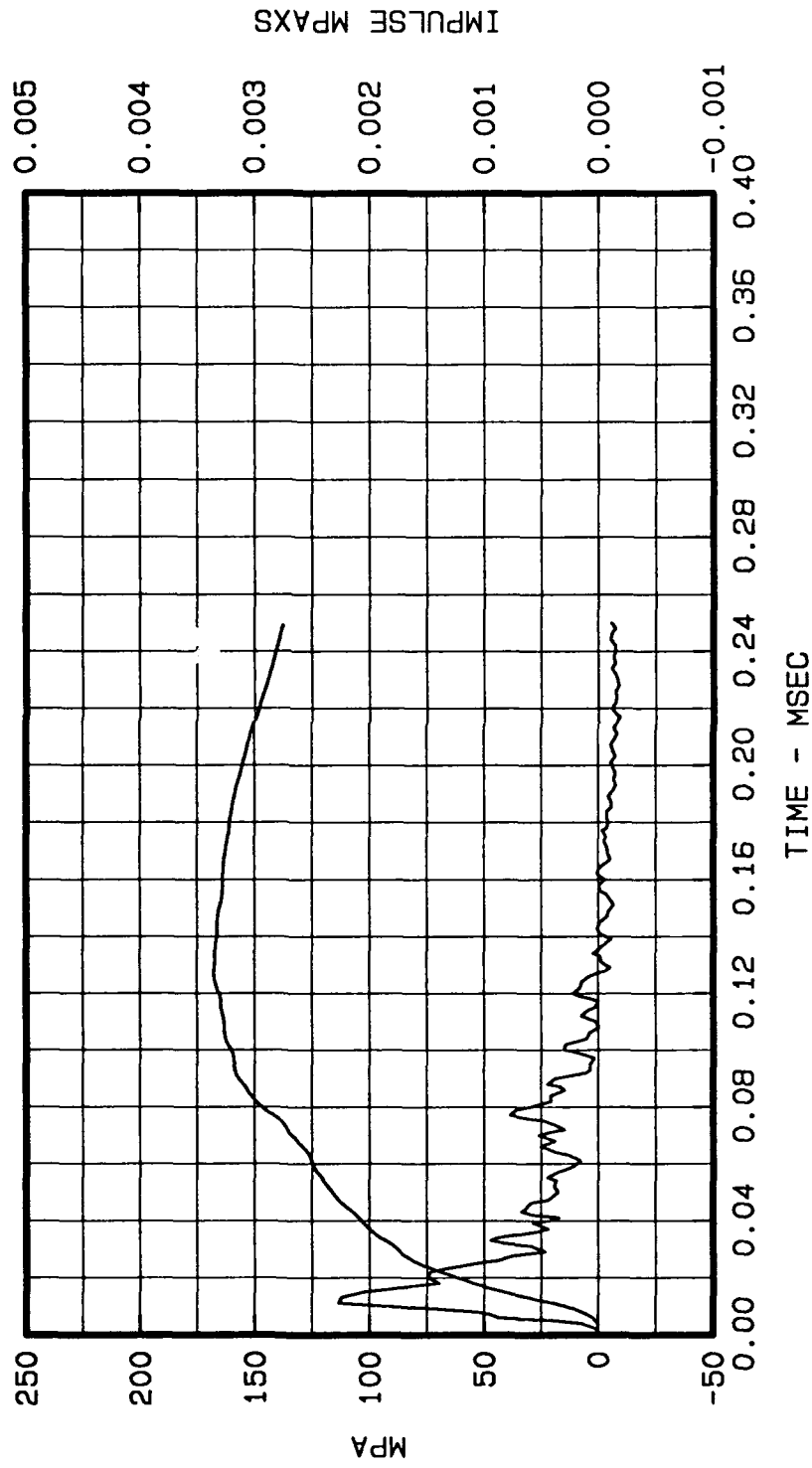


Figure B.9 WES Brick Model Test 2: Gage AB-9, chamber pressure-time history on side wall 25 cm from front of chamber.

Digital Gage
Array Size: 200050
Stop at 0.37
Cal val 80000
Deflection 1525

MUST AB-10

Model Underground Storage Test
Test 2

1000 KHZ 5-NOV-90

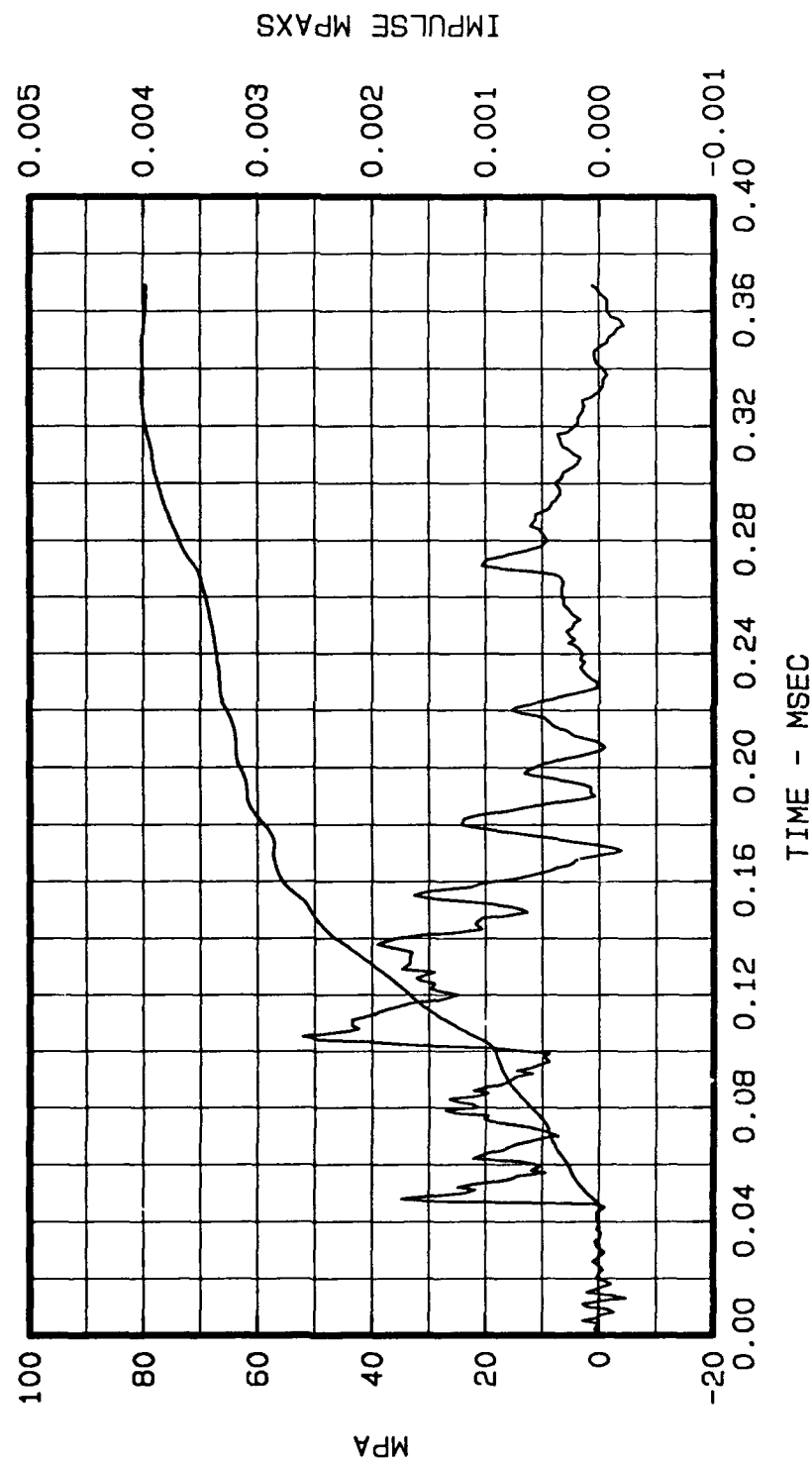


Figure B.10 WES Brick Model Test 2: Gage AB-10, chamber pressure-time history on side wall 24 cm from rear of chamber.

Digital Gage
Array Size: 200050
Cal val 3894.3
Deflection -1540

MUST GM-1

Model Underground Storage Test

Test 2

1000 KHZ

30-OCT-90

CBS 0.300 2 3

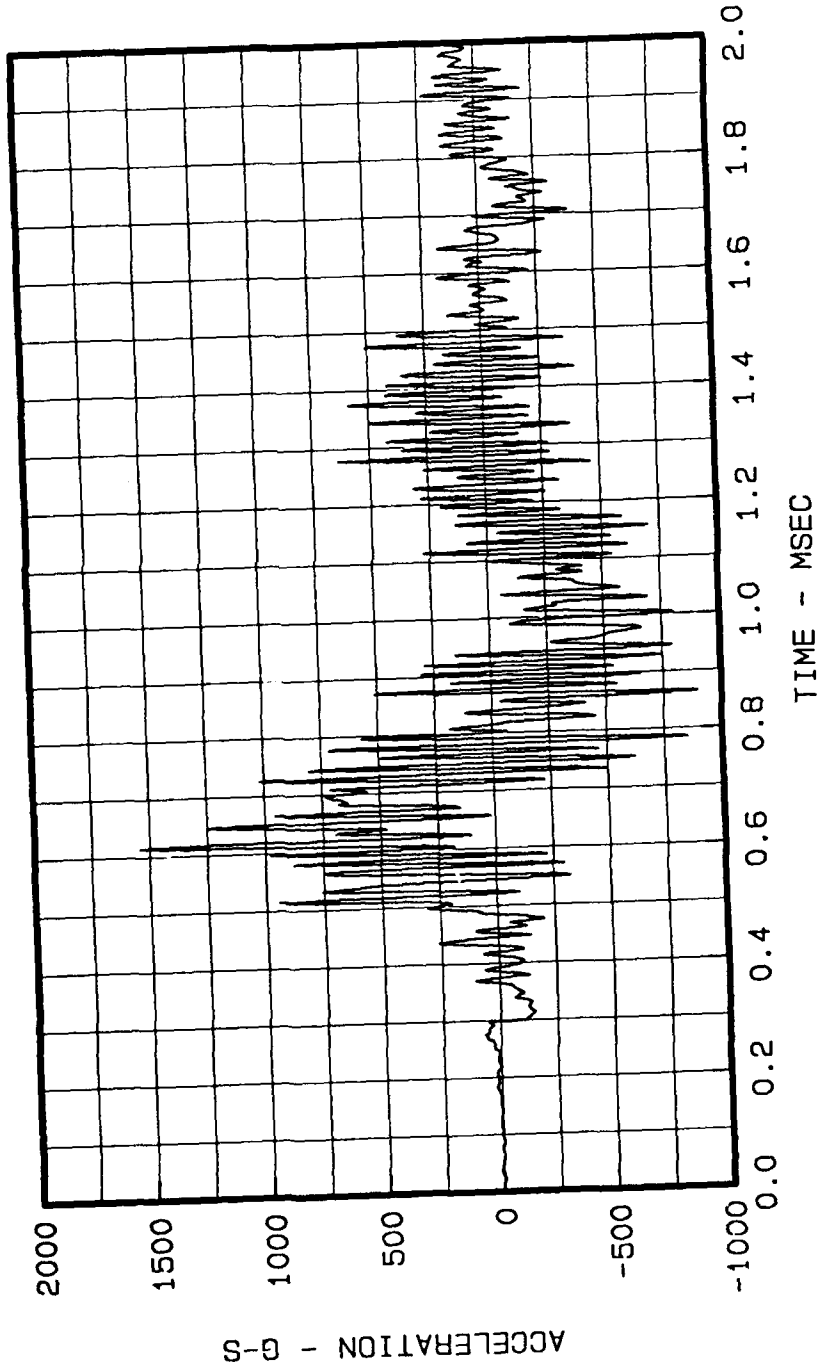


Figure B.11 WES Brick Model Test 2: Gage GM-1, overburden acceleration-time history at 18.3 cm above chamber roof.

Digital Gage
 Array Size: 200050
 Cal vel 3834.3
 Deflection -1540

MUST GM-1
 Model Underground Storage Test
 Test 2
 1000 KHZ 30-OCT-90

CBS 0.300 2 3

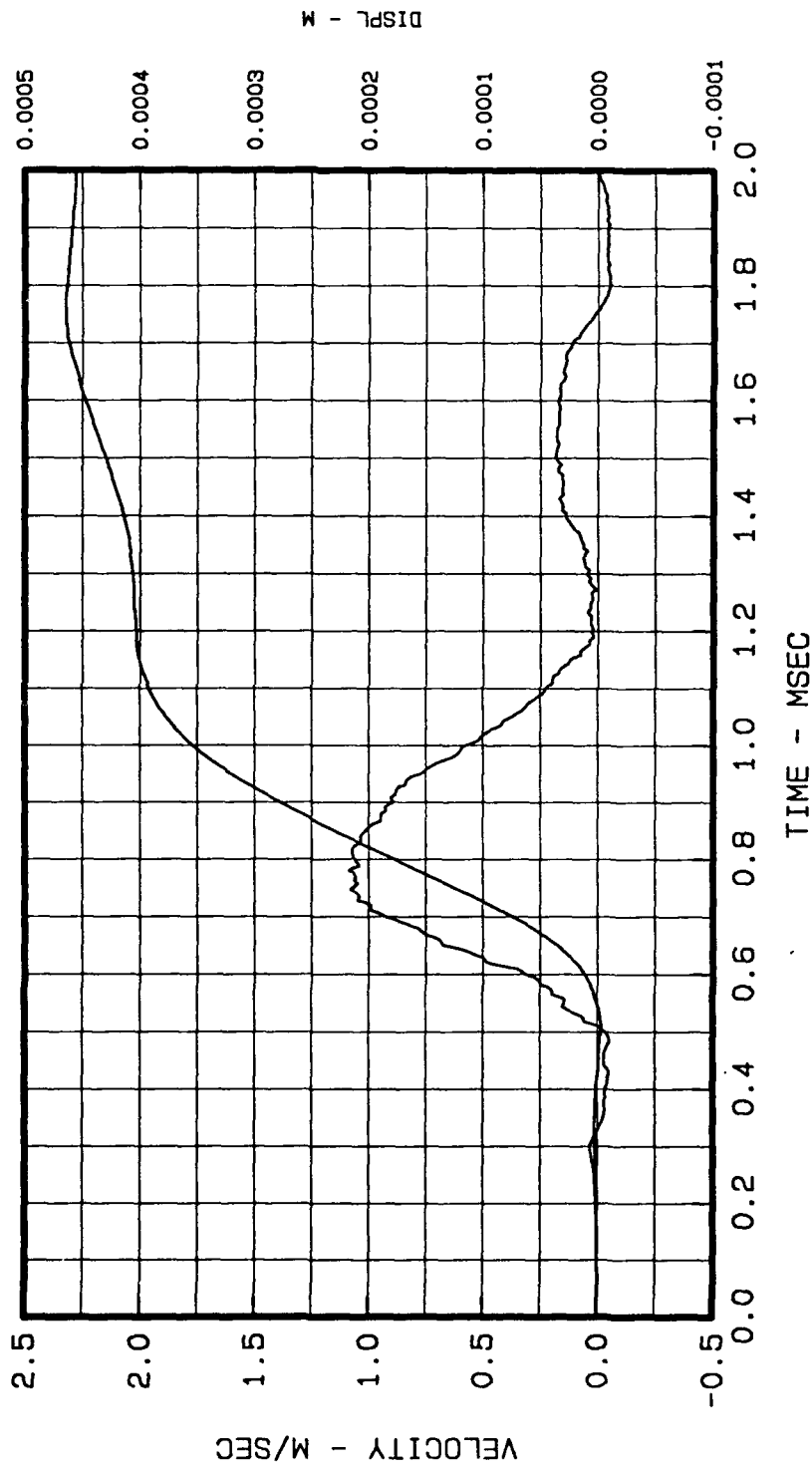


Figure B.12 WES Brick Model Test 2: Gage GM-1, overburden velocity-time history at 18.3 cm above chamber roof.

Digital Gage
 Array Size: 200050
 Polarity changed
 Cal val 3894.3
 Deflection -1557

MUST GM-2
 Model Underground Storage Test
 Test 2
 1000 KHZ 5-NOV-90

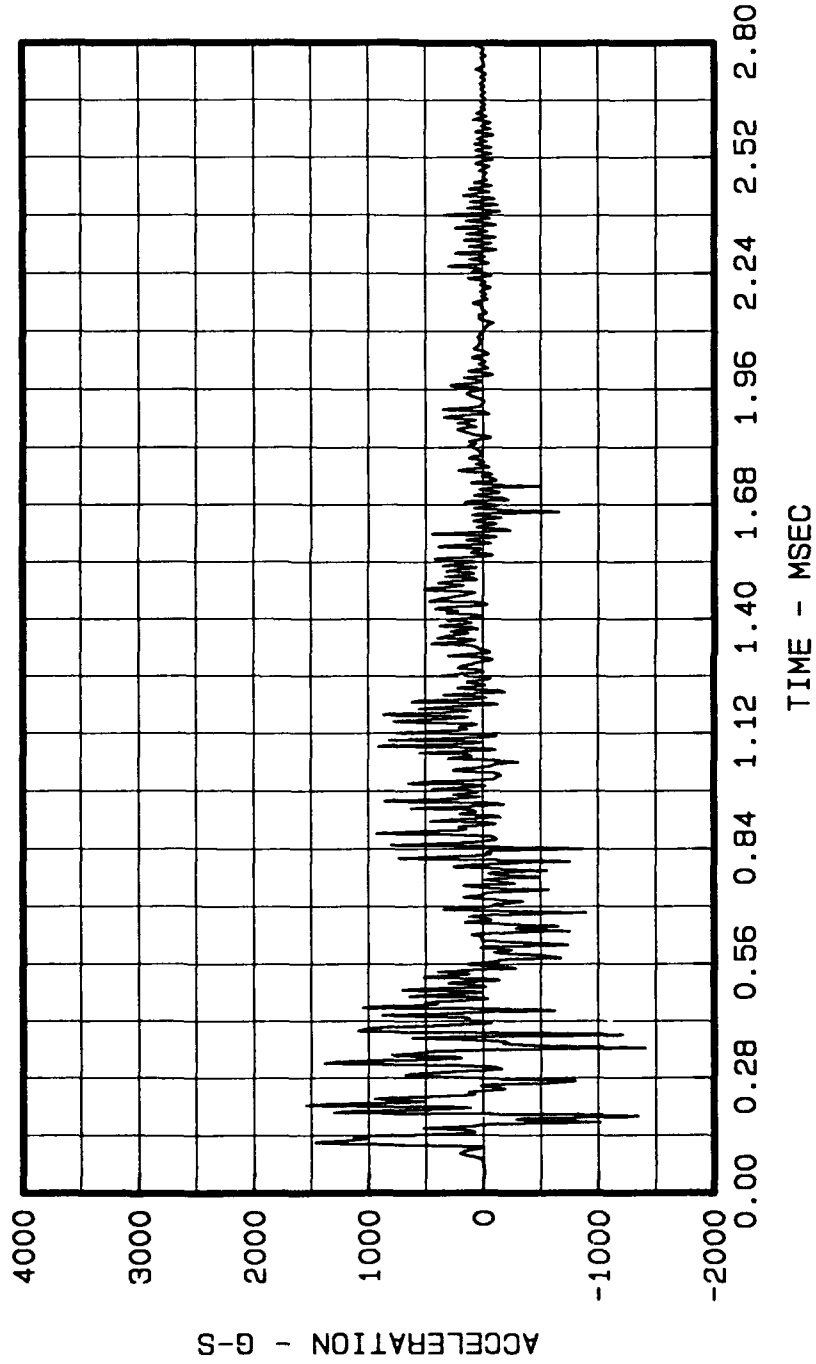


Figure B.13 WES Brick Model Test 2: Gage GM-2, overburden acceleration-time history at 36.6 cm above chamber roof.

Digital Gage
 Array Size: 200050
 Polarity changed
 Cal val 3834.3
 Deflection -1557
 MUST GM-2
 Model Underground Storage Test
 Test 2
 1000 KHZ 5-NOV-90

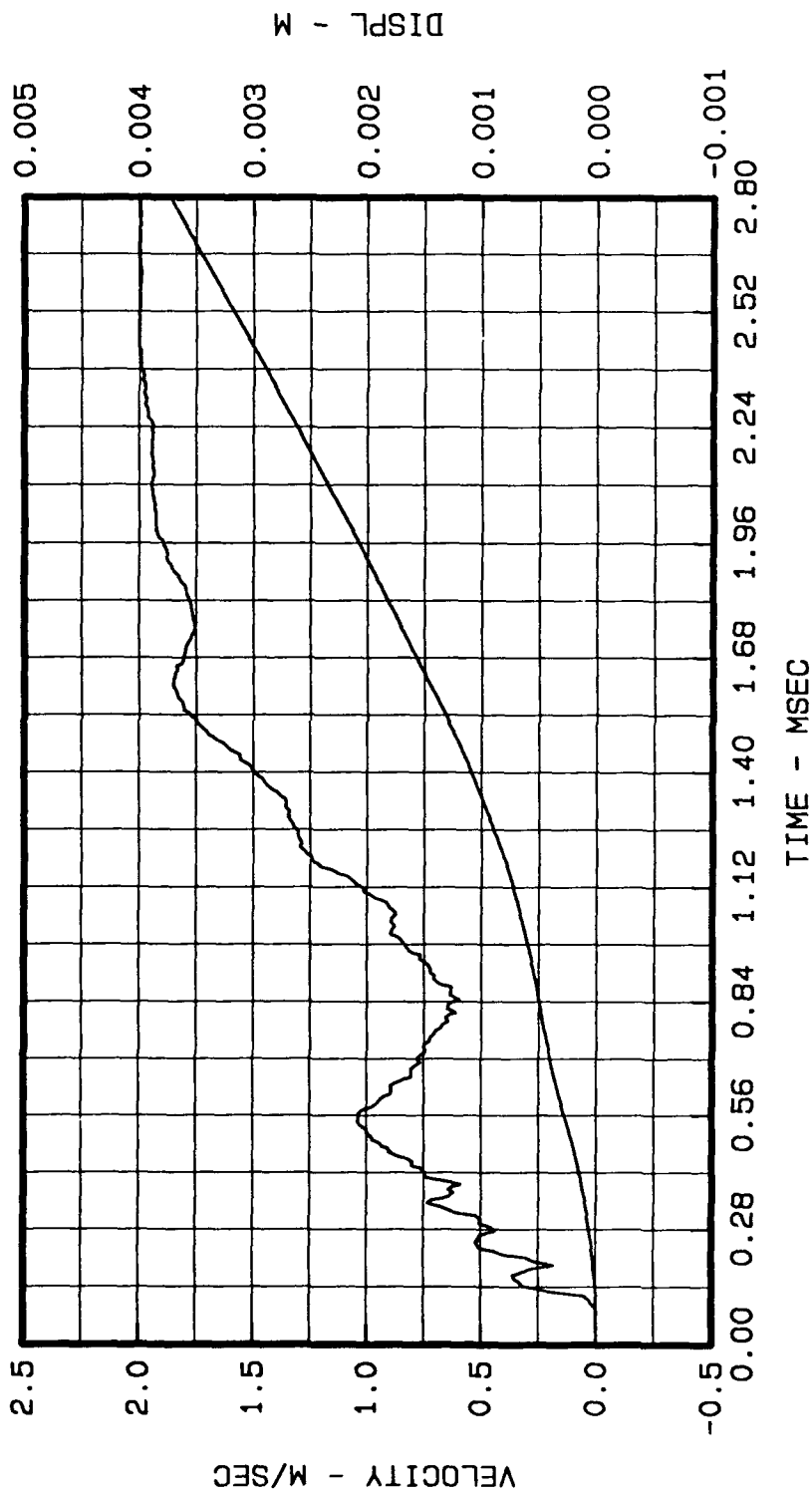


Figure B.14 WES Brick Model Test 2:; Gage GM-2, overburden velocity-time history at 36.6 cm above chamber roof.

APPENDIX C

AIRBLAST AND GROUND MOTION WAVE FORMS

Brick Model Test 3

Explosives Charge: 1.27 kg PETN

Chamber Loading Density: 60 kg/m³

Minimum Scaled Chamber Cover Depth: 0.79 m/kg^{1/3}

Digital Gage
 Array Size: 200050
 Cal val 1595.2
 Deflection -1030

MUST AB-1
 Model Underground Storage Test
 Test 3
 1000 KHZ 30-OCT-90

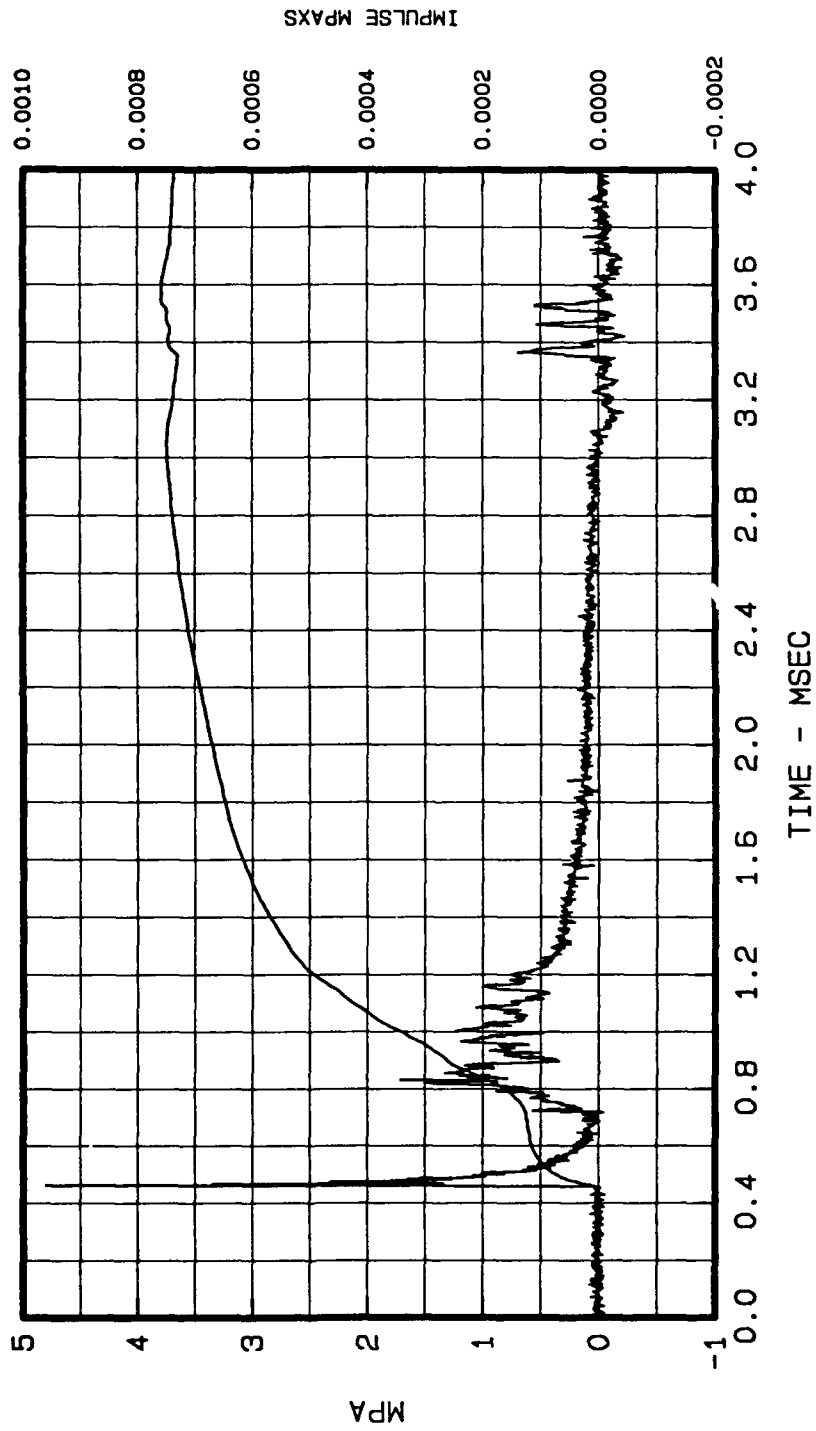


Figure C.1 WES Brick Model Test 3: Gage AB-1, free-field overpressure-time history at 20 cm from tunnel portal.

Digital Gage
 Array Size: 200050
 Stop at 1.54
 Cal val 285.200
 Deflection -1091

MUST AB-2

Model Underground Storage Test
 Test 3

1000 KHZ 30-OCT-90

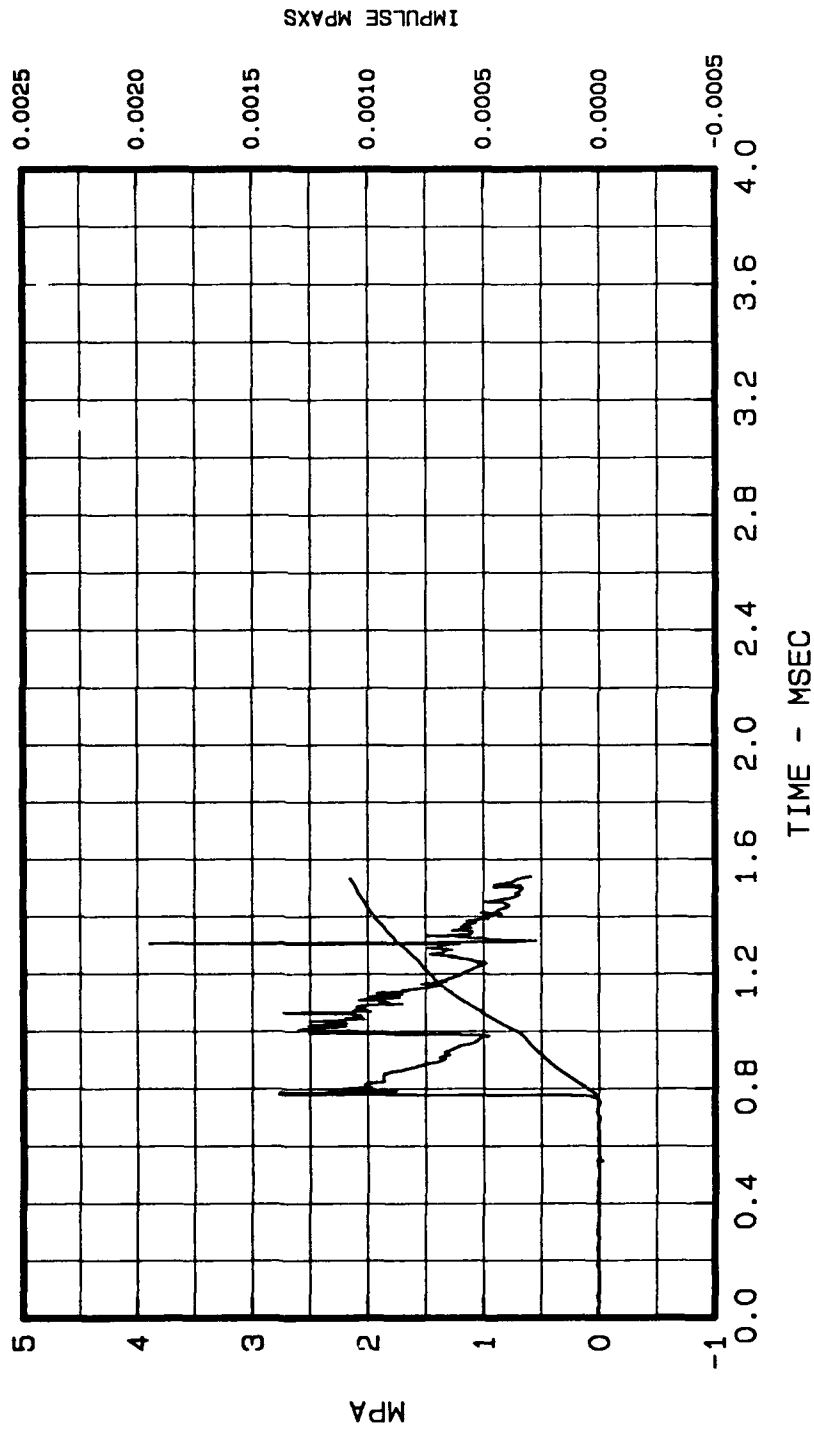


Figure C.2 WES Brick Model Test 3: Gage AB-2, stagnation pressure-time history at 20 cm from tunnel portal.

Digital Gage
Array Size: 200050
Cell val 6
Deflection -1039

MUST AB-5

Model Underground Storage Test
Test 3

1000 KHZ 5-NOV-90

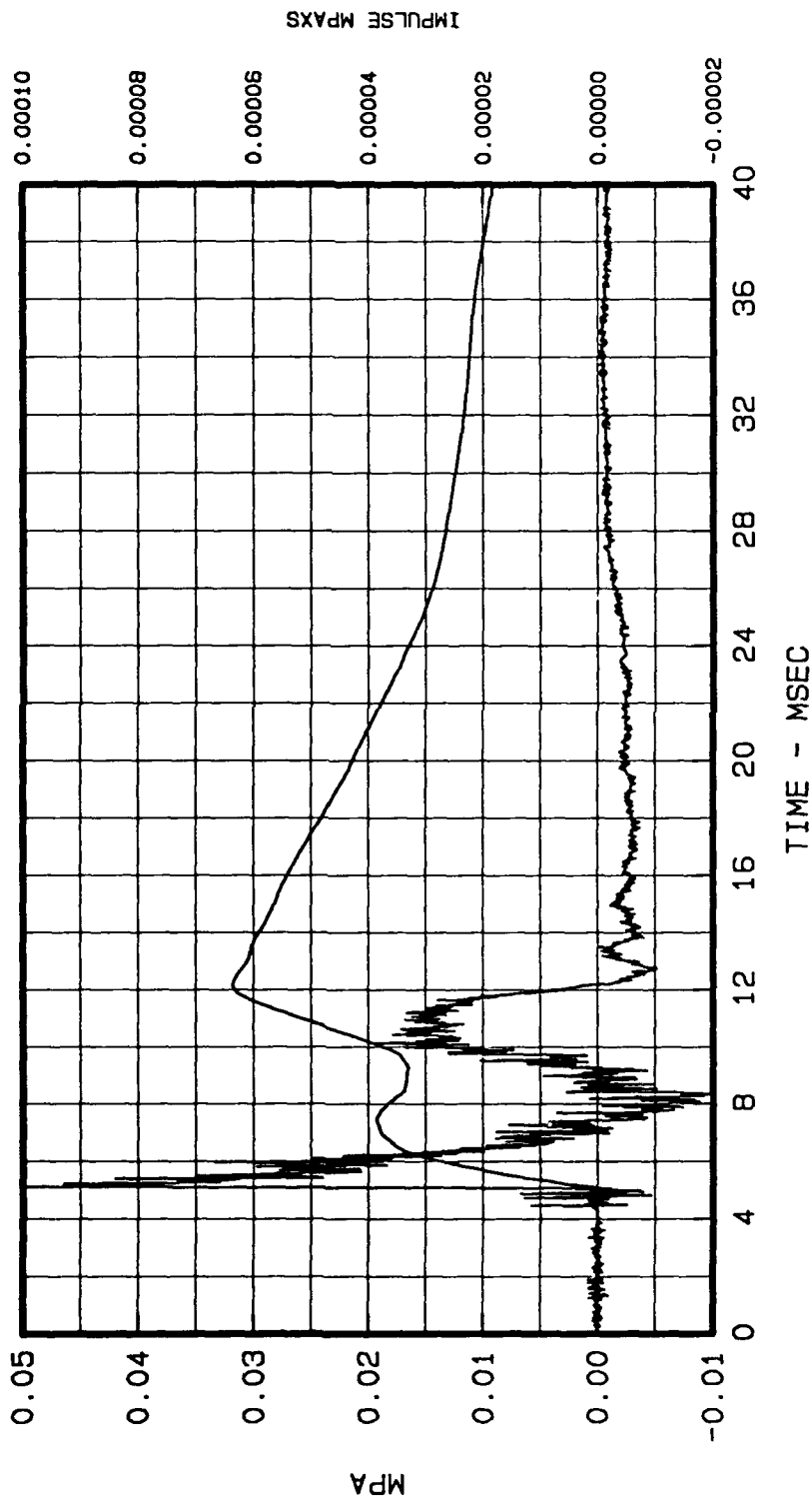


Figure C.5 WES Brick Model Test 3: Gage AB-5, free-field overpressure-time history at 3 m from tunnel portal.

Digital Gage
Array Size: 200050
Cal val 2.6
Deflection -1026

MUST AB-6

Model Underground Storage Test

Test 3

1000 KHZ 30-OCT-90

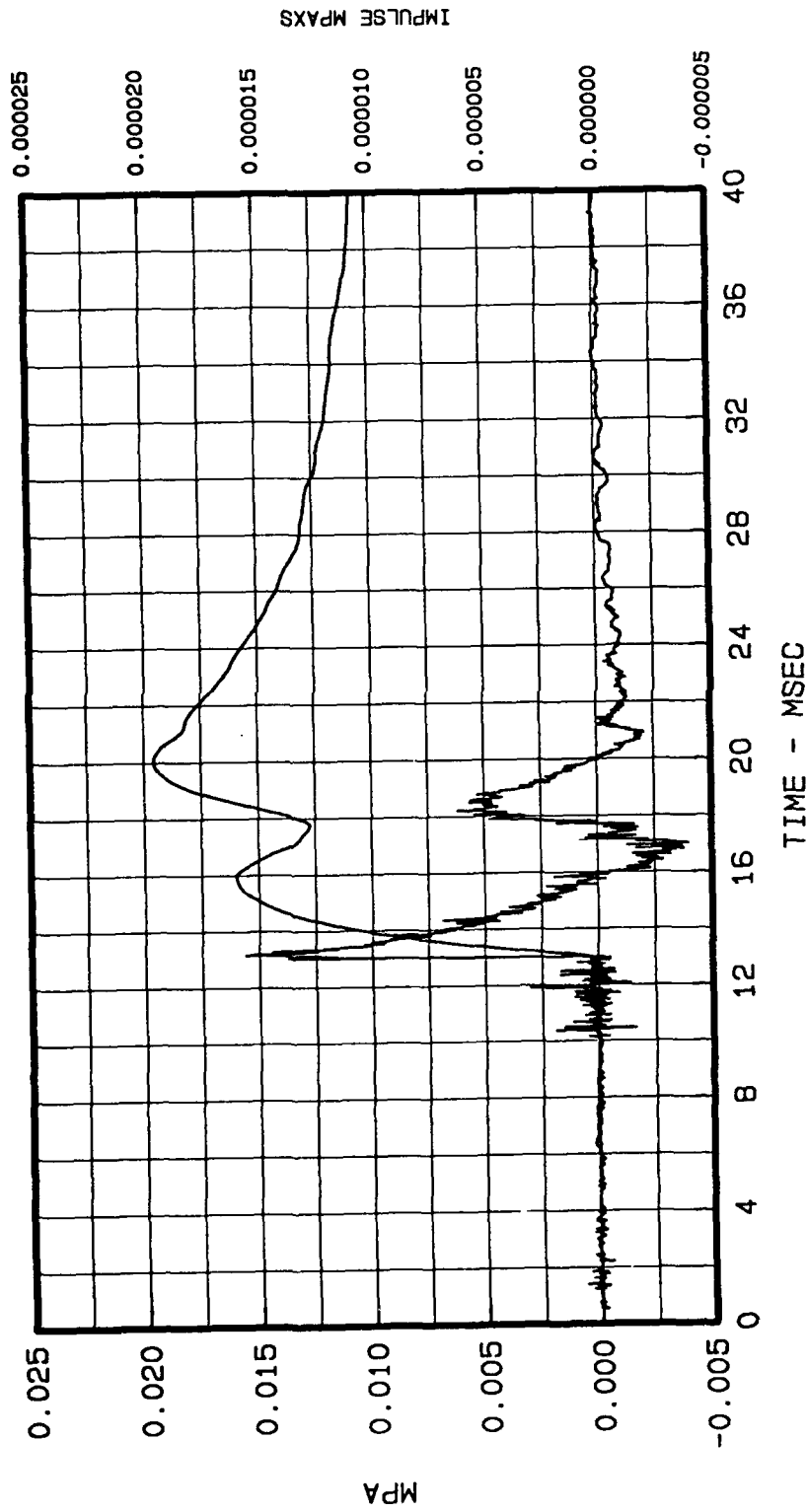


Figure C.6 WES Brick Model Test 3: Gage AB-6, free-field overpressure-time history at 6 m from tunnel portal.

Digital Gage
Array Size: 200050
Cal val 15915.4
Deflection -1029

MUST AB-7

Model Underground Storage Teat

Teat 3

1000 KHZ 30-OCT-90

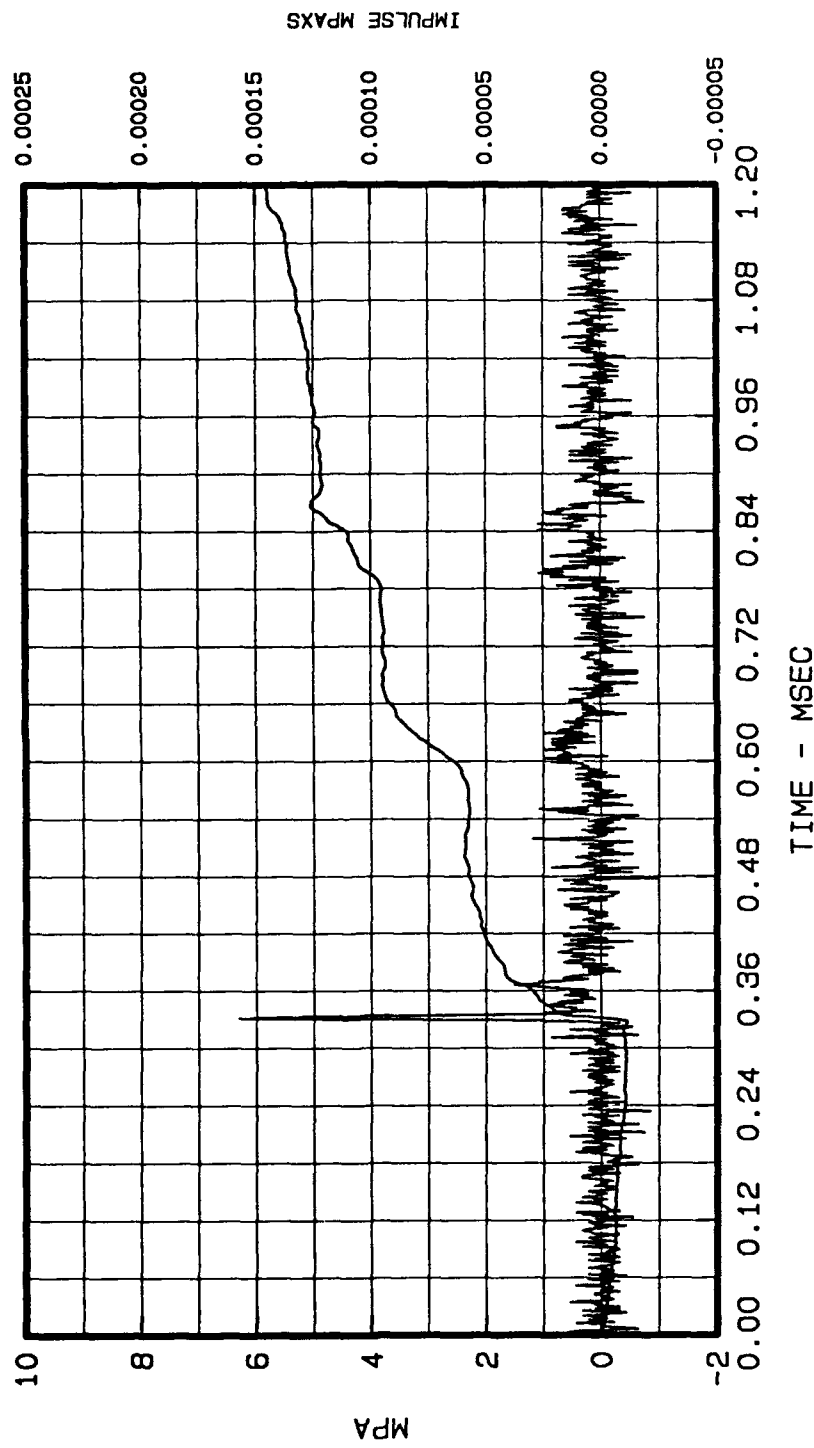


Figure C.7 WES Brick Model Test 3: Gage AB-7, access tunnel overpressure-time history at 10 cm from tunnel portal.

Digital Gage
Array Size: 200050
Cal val 15409.4
Deflection -1023

MUST AB-8

Model Underground Storage Test
Test 3
1000 KHZ 30-OCT-90

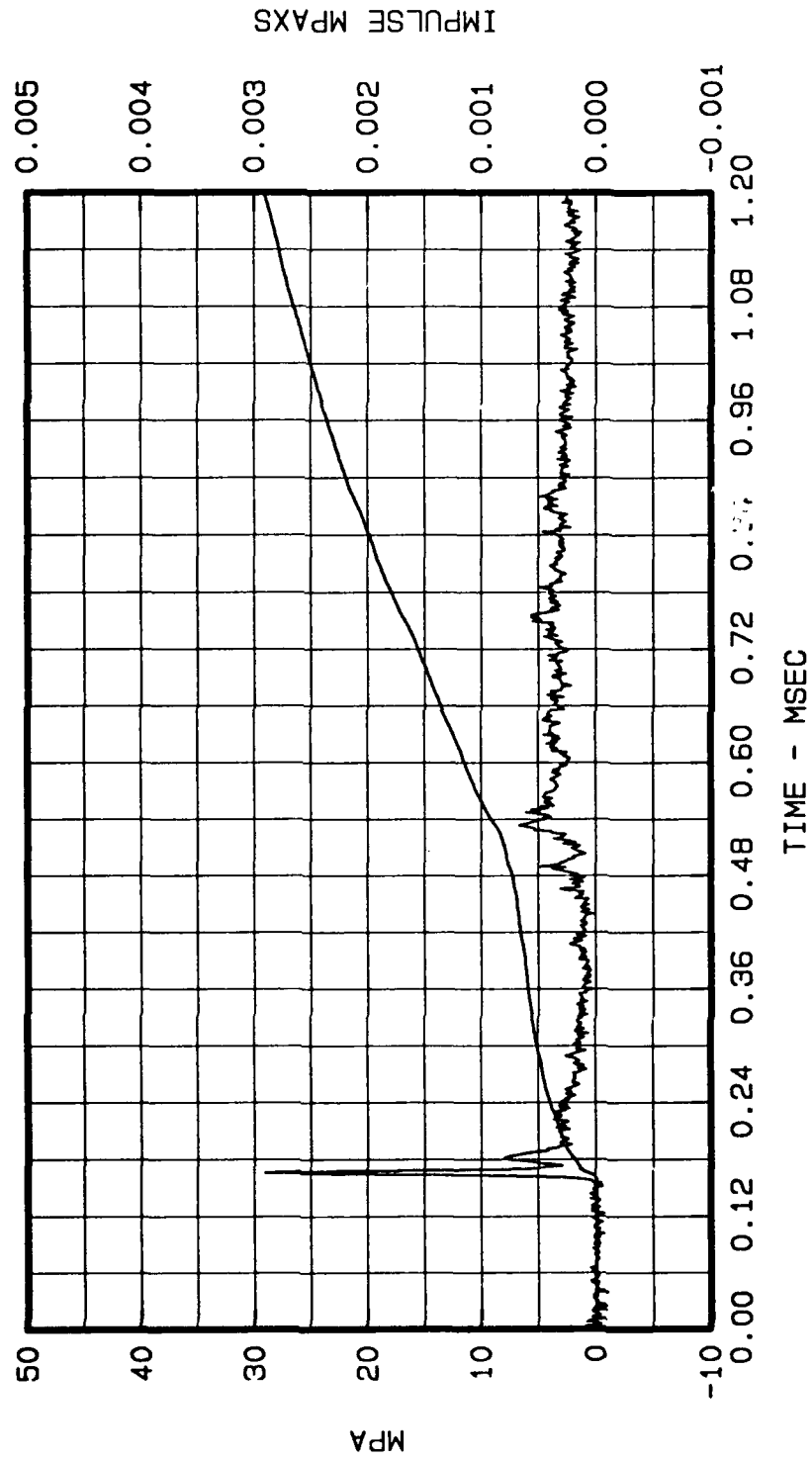


Figure C.8 WES Brick Model Test 3: Gage Ab-8, access tunnel overpressure-time history at 50 cm from tunnel portal.